



THE UNIVERSITY *of* EDINBURGH

Edinburgh Research Explorer

Angular gyrus involvement at encoding and retrieval is associated with durable but less specific memories

Citation for published version:

van der Linden, ML, Berkers, RMWJ, Morris, R & Fernandez, G 2017, 'Angular gyrus involvement at encoding and retrieval is associated with durable but less specific memories', *Journal of Neuroscience*.
<https://doi.org/10.1523/JNEUROSCI.3603-16.2017>

Digital Object Identifier (DOI):

[10.1523/JNEUROSCI.3603-16.2017](https://doi.org/10.1523/JNEUROSCI.3603-16.2017)

Link:

[Link to publication record in Edinburgh Research Explorer](#)

Document Version:

Peer reviewed version

Published In:

Journal of Neuroscience

General rights

Copyright for the publications made accessible via the Edinburgh Research Explorer is retained by the author(s) and / or other copyright owners and it is a condition of accessing these publications that users recognise and abide by the legal requirements associated with these rights.

Take down policy

The University of Edinburgh has made every reasonable effort to ensure that Edinburgh Research Explorer content complies with UK legislation. If you believe that the public display of this file breaches copyright please contact openaccess@ed.ac.uk providing details, and we will remove access to the work immediately and investigate your claim.



Research Articles: Behavioral/Cognitive

Angular gyrus involvement at encoding and retrieval is associated with durable but less specific memories

Marieke van der Linden¹, Ruud M.W.J. Berkers¹, Richard G. M. Morris² and Guillén Fernández¹

¹*Donders Institute for Brain, Cognition and Behaviour, Radboud University Nijmegen Medical Centre, 6500 HB, Nijmegen, The Netherlands.*

²*Centre for Cognitive and Neural Systems, The University of Edinburgh, EH8 9JZ, Edinburgh, United Kingdom*

DOI: 10.1523/JNEUROSCI.3603-16.2017

Received: 23 November 2016

Revised: 12 August 2017

Accepted: 17 August 2017

Published: 4 September 2017

Author contributions: Conceptualization, M.vdL., R.B., R.M., and G.F.; Investigation, M.vdL.; Writing — Original Draft, M.vdL.; Writing — Review & Editing, M.vdL., R.B., R.M., and G.F.; Funding Acquisition, G.F. and R.M.

Conflict of Interest: The authors declare no competing financial interests.

The authors thank Hester Breman for programming the sdmcalculator plug-in for BrainVoyager. This research was funded by an ERC Advanced Grant (268800) to G.F. and R.M. R.B. is currently affiliated with the Max Planck Institute for Human Cognitive & Brain Sciences, Leipzig, Germany. M.v.d.L. is currently affiliated with Máxima Medisch Centrum, Veldhoven, The Netherlands.

Correspondence: Dr. Marieke van der Linden, Donders Institute for Brain Cognition and Behaviour, Centre for Cognitive Neuroimaging, PO Box 9101, NL-6500 HB Nijmegen, The Netherlands. E-mail: marieke.vanderlinden@gmail.com

Cite as: J. Neurosci ; 10.1523/JNEUROSCI.3603-16.2017

Alerts: Sign up at www.jneurosci.org/cgi/alerts to receive customized email alerts when the fully formatted version of this article is published.

Angular gyrus involvement at encoding and retrieval is associated with durable but less specific memories

Marieke van der Linden^{*1}

Ruud M.W.J. Berkers¹Richard G. M. Morris²Guillén Fernández¹

¹. Donders Institute for Brain, Cognition and Behaviour, Radboud University Nijmegen Medical Centre, 6500 HB, Nijmegen, The Netherlands. ². Centre for Cognitive and Neural Systems, The University of Edinburgh, EH8 9JZ, Edinburgh, United Kingdom

*Correspondence: Dr. Marieke van der Linden, Donders Institute for Brain Cognition and Behaviour, Centre for Cognitive Neuroimaging, PO Box 9101, NL-6500 HB Nijmegen, The Netherlands. E-mail: marieke.vanderlinden@gmail.com

Abbreviated title: AG promotes durable but less specific memories

Words abstract: 139/250

Words intro: 670/650

Words discussion: 1498/1500

Number of figures: 8

Number of tables: 2

Acknowledgements

The authors thank Hester Brehman for programming the sdmcalculator plug-in for BrainVoyager. This research was funded by an ERC Advanced Grant (268800) to G.F. and R.M. R.B. is currently affiliated with the Max Planck Institute for Human Cognitive & Brain Sciences, Leipzig, Germany. M.v.d.L. is currently affiliated with Máxima Medisch Centrum, Veldhoven, The Netherlands.

The authors declare no competing financial interests.

25 **Abstract**

26 After consolidation, information belonging to a mental schema is better remembered, but such
27 memory can be less specific when it comes to details. A neuronal mechanism in line with this
28 behavioral pattern could result from a dynamic interaction that entails mediation by a specific
29 cortical network with associated hippocampal disengagement. We now report that in male and
30 female adult human subjects, encoding and later consolidation of a series of objects embedded in a
31 semantic schema was associated with a build-up of activity in the angular gyrus (AG) that predicted
32 memory 24h later. In parallel, the posterior hippocampus became less involved as schema objects
33 were successively encoded. Hippocampal disengagement was related to an increase in falsely
34 remembering objects that were not presented at encoding. During both encoding and retrieval, the
35 AG and lateral occipital complex (LOC) became functionally connected and this interaction was
36 beneficial for successful retrieval. Thus, a network including the AG and LOC enhances the overnight
37 retention of schema-related memories, and their simultaneous detachment from the hippocampus
38 reduces the specificity of the memory.

39

40 **Significance statement**

41 This study provides the first empirical evidence on how the hippocampus and the neocortex interact
42 dynamically when acquiring and then effectively retaining durable knowledge that is associated to
43 pre-existing knowledge, but they do so at the cost of memory specificity. This interaction is a
44 fundamental mnemonic operation that has been largely overlooked in memory research so far.

45

46

47 In time, most of the details of our experiences are forgotten. Some information is, however, retained
48 for a longer period of time and thought to be stored in neocortical networks that are separate from
49 the hippocampus (Scoville and Milner, 1957; Squire, 1986; Bontempi et al., 1999). This selectivity of
50 memory retention is the basis of the standard model of system-level consolidation (Alvarez and
51 Squire, 1994; Frankland and Bontempi, 2005). After consolidation, the medial prefrontal cortex
52 (mPFC) and mid-line cortical regions have been observed to be activated during memory retrieval in
53 rodents (Bontempi et al., 1999; Frankland et al., 2004; Maviel et al., 2004; Takehara-Nishiuchi et al.,
54 2006; Takehara-Nishiuchi and McNaughton, 2008; Goshen et al., 2011) and humans (Takashima et
55 al., 2006; Gais et al., 2007; Takashima et al., 2009; Bonnici et al., 2012).

56 Schemas provide a 'fast-track' into successful consolidation. Schemas are frameworks of
57 acquired knowledge that are implemented in the brain as networks of interconnected neocortical
58 representations (Wang and Morris, 2010). Schemas facilitate the assimilation of related new
59 information, leading to better retention (Bransford and Johnson, 1972; Tse et al., 2007; van Kesteren
60 et al., 2010b). The mPFC is more involved in processing memories congruent with a schema
61 compared to schema-incongruent memories (van Kesteren et al., 2010b; Tse et al., 2011; van
62 Kesteren et al., 2013b; van Kesteren et al., 2014; Brod et al., 2015). Initial evidence suggests that the
63 parietal cortex also participates in applying a schema to an experimental task (Hanson et al., 2007;
64 Sweegers et al., 2014; van Buuren et al., 2014).

65 This study investigates the possibility that the angular gyrus (AG) plays a key role in binding
66 sensory content into a schema. Within the ventral parietal cortex, the angular gyrus (AG) is optimally
67 located at the junction of visual, spatial, somatosensory, and auditory processing streams. These
68 sensory-motor attributes all converge in the AG, where the perceptual details are believed to be
69 abstracted (Fernandino et al., 2015) and bound together by semantic and conceptual associations
70 (Binder et al., 2009b). After consolidation, the AG recombines schema components into a single
71 memory representation (Wagner et al., 2015).

72 We sought to elucidate the roles of the MTL, mPFC, and AG in the encoding and
73 consolidation of new information, followed by the later retrieval of recent (within-session) and
74 remote (24 hr. earlier) schema-associated memories. During encoding, a series of four object
75 photographs were presented in sequence (Figs. 1 & 2). In the schema condition these objects were
76 all related to a real-world semantic schema (e.g. horse, spurs, boots, and a cowboy's hat). If the AG is
77 involved in processing schema-related objects, successive presentation of these objects will
78 modulate activity in the AG in a different way than a series of semantically unrelated objects. At the
79 same time, the build-up of a schema could lead to disengagement of the hippocampus during
80 encoding. An additional condition was included where the last object of the set was incongruent
81 with the schema (e.g. a Christmas tree instead of the cowboy's hat). We expected the AG to respond
82 differently to the final object based on its incongruence with the preceding object set. Finally, we
83 also considered the implications of schemas with respect to subsequent retrieval. Shimamura (2011)
84 suggested that the AG links "episodic features with long-term memory networks", an idea that leads
85 to the prediction that such networks (schemas) will be recruited as the schema is built up. This
86 dynamic process could in turn influence the encoding and/or consolidation of schema-related
87 information, and that the AG should differentiate between subsequent retrieval of objects that were
88 embedded in a schema during encoding compared to objects that were not.

89 The neocortical regions that likely support lasting memory representations include brain
90 areas involved in the original processing of the stimulus at encoding (Tulving and Thomson, 1973;
91 Nyberg et al., 2000; Danker and Anderson, 2010), and in the case of visually presented objects, these
92 include ventral visual areas such as the lateral occipital complex (LOC). To test our prediction that
93 the AG would be functionally connected to visual representation areas during encoding and item
94 recognition, and that successful linking to these object representations would be beneficial to
95 memory retention, we included a functional localizer scan.

96

97 **Materials and Methods**

98 *Participants*

99 In total, 31 participants participated in the experiment. For 7 participants, the data were excluded
 100 from the final analyses for the following reasons: Two participants did not complete the study; one
 101 participant moved 12 mm during scanning; one participant fell asleep during encoding on the second
 102 day; three participants displayed memory performance that did not exceed chance level. The
 103 presented results stem from a dataset with 24 right-handed participants (2 males, 22 females - mean
 104 age: 23.5 years, range 18-30 years). All participants were neurologically healthy and were paid for
 105 their participation (10 euro per hr., with an additional 2 euro per every 10% that they scored above
 106 50%, i.e. chance level). For two out of 24 participants, the data sets were incomplete because of
 107 scanner malfunction during one of the encoding sessions. For these incomplete data sets, the data
 108 were adjusted in further analyses (i.e. the objects they did not see during encoding were removed
 109 from the item recognition test, maximum of 20% of the trials).

110

111 *Stimuli*

112 Stimuli consisted of color photographs of objects. These photographs were taken from the Hemera
 113 Object Database and Google image search. Objects were shown on a white background and were
 114 made to fit exactly in a box of 300x300 pixels while keeping their aspect ratios intact.

115

116 In our experiment, a schema was defined as a group of objects that are all related to each other
 117 through a semantic theme. More specific, a schema consisted of four pictures of objects (a quartet)
 118 from the same theme (see Figure 1a for an example of a “knight” schema). In total we used 100
 119 themes, consisting of places, characters, seasons, sports, events, holidays, professions, rooms,
 120 countries etc. The schemas were created by selecting sets of 4 objects that ostensibly fitted within a
 121 theme, based on a separate preparatory study (N=20). In this, participants were presented with a
 122 theme, written on a screen, and they were instructed to type in the names of at least 10 objects that
 123 they associated with this theme. The nine objects that were mentioned most frequently were used

124 to form two quartets per schema and one related new object (schema-based lure). Schema-strength
 125 of an object was identified as the proportion of participants that mentioned an object within a given
 126 theme. When creating the quartets, the schema-strength of the objects was taken into account such
 127 that this was divided equally over positions in the quartets (on average 27.5% for each of the four
 128 positions). A second type of quartet (incongruent) was constructed by shuffling the Schema quartets'
 129 final objects around so that this object did not fit with the other three objects in the quartet
 130 anymore (Fig. 1a). We also constructed 100 No schema quartets in which there was no a priori
 131 association between the objects (see also Fig. 1a for an example). The schema consistency of the
 132 schemas - and the absence of schema for the No schema quartets - was confirmed in a second
 133 preparatory study (N=20). A different group of participants was asked to press a button during serial
 134 presentation of the objects in the quartets as soon as the schema was known to them. For the No
 135 schema quartets, there were no reports of schemas by the participants, whereas for the Schema
 136 quartets the average number of participants that correctly reported the schema was 90% (15% SD).

137

138 *Image acquisition*

139 During encoding and retrieval whole-brain images (T2*-weighted multi-echo planar imaging, 39
 140 slices, 2 mm thick with 0.5 mm gap, repetition time = 2190 ms, in plane resolution = $2.5 \times 2.5 \text{ mm}^2$,
 141 four echo times: TE1 = 9.4 ms, TE2 = 21.9 ms, TE3 = 34 ms, TE4 = 47ms, flip angle = 90° , field of view =
 142 21.2 cm) were acquired on a 3T whole body MR scanner (MAGNETOM Skyra by Siemens Medical
 143 Systems, Erlangen, Germany). Fat saturation was turned off. During the functional localizer scan, we
 144 acquired whole-brain images (echo planar imaging, 45 slices, 2 mm thick with 0.5 mm gap, repetition
 145 time = 2390 ms, in plane resolution = $2.5 \times 2.5 \text{ mm}^2$, TE = 30 ms, flip angle = 90° , field of view = 21.2
 146 cm). In addition, a high resolution structural T1-weighted 3D magnetization prepared rapid
 147 acquisition (MPRAGE) gradient echo sequence image was obtained after the functional scan (192
 148 slices, voxel size = $1 \times 1 \times 1 \text{ mm}$).

149

150 *Experimental Design and Statistical Analysis*

151

152 Design and procedure

153 Participants were scanned on two consecutive days (see Figure 2a). On the first day, they encoded
 154 (for 53 min) the first set of objects (called the “remote” condition by virtue of its distance from
 155 retrieval the next day). Before they started with this first encoding session, they were scanned using
 156 a functional object localizer. After 24 hr. (sleep duration was on average 7.9 hr. with a standard
 157 deviation of 45 min), they returned to the lab for the second encoding session (“recent” condition,
 158 53 min). After the second encoding session, they had a short break outside the scanner and then
 159 returned inside the scanner for the item recognition memory task probing memory for both remote
 160 and recent items (58 min).

161

162 Functional localizer

163 An independent functional localizer was included to allow us to investigate at a later time point
 164 whether PPI connectivity maps from memory areas overlapped with visual representation areas that
 165 preferentially respond to objects. The participants were told what the purpose of the localizer scan
 166 was and that they need not memorize the pictures they were shown. We used a block design using
 167 32 photographs of common objects (unrelated to the schemas in the main experiment) and 32
 168 scrambled pictures from a standard functional localizer task to localize the lateral occipital complex
 169 (LOC, (Malach et al., 1995). Images had grey backgrounds and measured 500 x 500 pixels. Images
 170 were randomly assigned to blocks of 17 images (each image was displayed for 400 ms and followed
 171 by a blank screen of 600 ms). Each block lasted 16.4 seconds. Within each block 16 images were
 172 unique and one image was repeated. The participants were instructed to detect this repetition by
 173 pressing a button with the index finger of the right hand. Each block was followed by a blank screen
 174 interval of 10 seconds. Each image was presented twice to the subject, but within different blocks.
 175 Four blocks of objects and four blocks of scrambled objects were presented. The localizer run lasted
 176 3.5 mins.

177 Encoding

178 During each of two memory encoding sessions (called ‘remote’ and ‘recent’ in chronological order of
179 presentation), 150 quartets were serially presented to the participants, one object after the other,
180 see Figure 1a and Figure 2b. Quartets belonged to three schema conditions: First, the Schema
181 condition, in which all objects in the quartet belong to one theme. Second, the Incongruent
182 condition, in which the final item of the quartet was incongruent with the theme provided by the
183 first three items. Third, the No schema condition, where there was no obvious association (schema)
184 between the objects. The participants were instructed to remember all objects and quartets. They
185 were also told that during the final memory test they would be presented with very similar lures so
186 that they should try to remember as many details as possible. Simultaneously, they were asked to
187 indicate for each object whether it would fit inside a shoebox. They responded “yes” and “no” with
188 their index and middle finger of their right hand. Participants were told that memorizing the objects
189 and quartets had priority over the “shoebox task”. A black fixation cross was visible on screen
190 throughout the encoding session and this fixation cross changed to red to signal the start of a new
191 quartet. The red fixation cross was presented for 500 ms. The objects were presented for 1500 ms
192 and the inter-stimulus interval was 3.5 s on average. All inter-stimulus intervals were jittered
193 between 1.5 and 5.5 s. During each encoding session they were presented with 600 objects, so
194 across the two encoding sessions participants memorized 300 quartets containing 1200 objects. We
195 installed a few safe-guards to minimize memory to specific items (that arise from some objects being
196 more memorable than others): First, the quartets were counterbalanced between subjects over
197 remote and recent encoding sessions. Second, targets and lures were counterbalanced over subjects.
198 Third, the quartet’s final objects were semi-counterbalanced over schema conditions, as the objects
199 in the fourth position of each quartet could not be swapped between Schema and No Schema
200 quartets. As such, final objects were counterbalanced over Schema and Incongruent conditions
201 across subjects, and a second counterbalancing was performed in terms of the assignment of objects
202 to the Incongruent and No Schema Conditions.

203

204 Retrieval

205 Retrieval was tested by an item recognition memory task. The experiment started with 3 practice
206 trials with objects that were new and not seen before (to familiarize the participant with the timing
207 of the events and the task). During the item recognition task, the participants were presented
208 sequentially with photographs of objects in a pseudorandom order. The quartets' final items were
209 presented as old targets (Figure 1b). A perceptually similar lure was included for each target (Fig 1b).
210 Half of the targets were presented before the lure, and half after the lure. Moreover, the spacing in
211 time between a target and its lure was maximized. In addition, fifty objects that were related to a
212 schema, but that were not presented during encoding, served as new Schema objects during
213 retrieval (Fig 1b). There were another 50 objects that were new and were not related to the
214 presented schemas, the new No schema objects. This resulted in a total of 700 objects that were
215 presented to the participants (see Fig 2c for an overview of all conditions).
216 After the presentation of a fixation cross (500ms), each object was presented for 1500 ms, Figure 2b.
217 Subjects rated their memory for the objects using a confidence scale, ranging from 1 (very surely old)
218 to 6 (very surely new). Half of the participants responded "old" with their index, middle, and ring
219 finger of their right hand and responded "new" with their index, middle, and ring finger of the left
220 hand and this was reversed in the other half of the participants. After a jittered interval (average =
221 3.5 s, range: 1.5 – 4.5 s), during which the confidence levels were displayed on screen, the next
222 object was presented.

223 After the retrieval session the participants filled in a short questionnaire asking them about
224 strategies used during encoding (90% reported using the schemas during encoding) and retrieval (17%
225 reported using the schemas during retrieval) and the amount of sleep on the previous night (on
226 average 8 hr.).

227

228 Behavioral data analyses

229 For each subject the proportion of hits (“old” responses to old objects), misses (“new” response to
 230 old objects), correct rejections (“new” response to new objects and similar lures), false alarms (“old”
 231 response to new objects and similar lures), and “no responses” were calculated per condition as well
 232 as the confidence levels and response times for each of these variables. Trials were included at all
 233 levels of confidence, because there was above chance memory performance at all confidence levels.
 234 To account for response bias, we subtracted the proportion of false alarms made when presented
 235 with the New No schema objects, from respectively the proportions of Schema, No schema, and
 236 Incongruent hits (to targets) and false alarms (to lures). Proportion of hits minus false alarms and
 237 response times were tested in two (separate) multivariate analyses of variance (MANOVAs) with 2
 238 factors: Schema condition (with 3 levels: Schema, Incongruent, and No schema) and Study-test delay
 239 (with 2 levels: Remote and Recent). Additional differences between conditions were tested using
 240 paired-samples and one-sample *t*-tests. All reported *p*-values are two-tailed. Alpha was set to 0.05.

241

242 MRI data analyses

243 The multi-echo fMRI data were processed using in-house software written in Matlab 7.5 (The
 244 Mathworks, Inc., Natick, MA, USA), which used the first 29 scans of the session (during which the
 245 experiment had not yet commenced) to calculate the optimal weighting of echo images for each
 246 voxel (i.e. by using a weighted measure of the contrast- to-noise ratio for each echo/scan). Motion
 247 correction was performed with reference to the first echo and the realignment parameters were
 248 applied to the other echoes by using iterative rigid body realignment. Next, calculations of optimal
 249 echo-weight for each voxel were used to combine multi-echo fMRI data into single images. The
 250 combined images were further processed using BrainVoyager QX (by Brain Innovation, Maastricht,
 251 The Netherlands). Images were slice-time corrected (using sinc interpolation). Co-registration of
 252 functional and 3D structural measurements was computed by relating T2*-weighted images and the
 253 T1-weighted MPAGE measurement, which yields a 4D functional data set. Structural 3D and

functional 4D data sets were transformed into Talairach space (Talairach and Tournoux, 1988) and spatially smoothed with a Gaussian kernel (FWHM = 8 mm).

The expected BOLD signal change was modeled using a gamma function (tau of 2.5 s and a delta of 1.5) and convolved with each presented object (Boynton et al., 1996). Regressors were time-locked to the onset and duration of the presentation of the objects. Data were corrected for serial correlation using the AR2 method and a percent signal change transformation was performed before statistical analysis. Statistical analyses were performed using the general linear model. For the encoding sessions we modeled the three conditions (Schema, Incongruent, and No schema) separately and subsequently remembered or forgotten separately. This means that all objects in a quartet were categorized as to whether the final object was remembered or forgotten (e.g. Condition1_Object1_Remembered, Condition1_Object2_Remembered, Condition1_Object3_Remembered, Condition1_Object4_Remembered). In the encoding sessions, the contrasts included only the final objects from the quartets. For the contrast between remembered and forgotten items, the items that were forgotten were collapsed across schema conditions, this ensured more trials in the forgotten conditions and we presume the same process for forgetting in all conditions (e.g. Schema remembered > Schema forgotten + No Schema forgotten + Incongruent forgotten).

We also constructed a parametric model in which the four objects within a block were given parametric weights (-1.5, -0.5, 0.5, and 1.5) and, per condition, the blocks were also divided depending on whether the final objects were subsequently remembered or forgotten. For the retrieval session we modeled the first 3 trials (not uniquely part of any condition: “warm-up” trials), hits, misses, false alarms and correct rejections separately for Schema, Incongruent, and No schema remote and recent objects, and to new No schema and new Schema objects, in total 29 regressors. Random-effects group analyses were performed using the analyses of variance (ANOVA) to test for interactions. The first analysis consisted of a random effects ANOVA with 3 factors: Schema

279 Condition (Schema, No schema, Incongruent), Study-test delay (Recent, Remote), and Memory (Hits,
280 Misses).

281 In addition, in all models, six derivatives of the realignment parameters were included as
282 well as regressors for spikes related to motion (one regressor per spike). Furthermore, *t*-tests were
283 used to test contrasts between different conditions. Results were thresholded at the voxel level at p
284 < 0.001 and corrected using Monte Carlo cluster threshold correction completed over 1000
285 iterations. Small Volume Correction was applied to the ventro-medial prefrontal cortex using False
286 Discovery Rate correction on the voxels that were included in an anatomical mask of Brodmann
287 areas 32 and 24. Significantly activated clusters in mPFC and angular gyrus (AG) were selected for a
288 more sensitive region of interest (ROI) analysis. For the ROI analyses the beta values were extracted
289 from all voxels within the ROI and averaged over ROI, subject, and condition. The ROI time courses
290 were standardized, so that beta-weights (regression coefficients) of predictors, as indices of effect
291 size, reflect the BOLD response amplitude of one condition relative to the variability of the signal.
292 Beta-weights were obtained for all voxels within these regions of interest, per subject and per
293 condition. Differences between the subject-averaged beta-weights were investigated by paired *t*-
294 tests with a threshold set at $p < 0.05$. All *t*-tests were two-tailed.

295 Finally, functional connectivity analyses (PPI) were conducted to determine the interactions
296 between physiological data in terms of the psychological processes of the experiment (Friston et al.,
297 1997). PPI methodology followed the steps first described in Friston et al. (1997) and was
298 implemented using a BrainVoyager plugin (sdmcalculator v0.2). For the PPI analysis on the retrieval
299 data, the seed-region we used was the AG region that was found in the Schema > No schema
300 contrast during retrieval. The time course was extracted and averaged across all voxels from this
301 area for each subject. As the psychological regressor, we used the contrast Schema remote hits (+1)
302 and No schema remote hits (-1). For a second PPI analysis, using the left parietal ROI, we used the
303 same methodology. As the seed, we used the areas found in the contrast Schema > No schema and
304 extracted per subject the time course from all voxels. The psychological contrast was the same

305 contrast as used for the previous PPI. To test for a general effect of correct responses on
 306 connectivity to the lateral occipital complex (LOC) we also calculated a PPI for remote No schema
 307 hits (+1) versus recent No schema hits (-1). For the PPIs on the encoding data we used as a seed the
 308 AG region that was active in the remote (Schema > No schema) > recent (Schema > No schema) and
 309 the LOC region from the functional localizer that was active for Objects > Scrambled.

310

311 To investigate the behavioral relevance of the connectivity between the seed and target areas, we
 312 performed a correlation analysis at the group-level (using Pearson's r) on the extracted PPI beta-
 313 values from the ROI with the behavioral measures: remote Schema hits, remote schema effect
 314 (Schema minus No Schema), and remote Schema false alarms. We also calculated correlation with
 315 behavioral measures (hits minus the false alarms to new No schema objects) and the schema build-
 316 up in the angular gyrus. Schema build-up was measured by subtracting beta-values to object four
 317 minus object two (the moment at which a schema can first be detected). The difference between
 318 two correlations was tested using software from Lee and Preacher (2013), available online.

319

320 **Results**

321 ***Behavioral data***

322 An important property of schema-based memories is that there is a behavioral benefit i.e. better
 323 memory retention for schema-related memories as compared to no-schema memories. Although
 324 this schema effect can be apparent immediately for associative memory, other studies have found
 325 that the difference between schema and non-schema-based item recognition is largest after a
 326 period of consolidation (van Kesteren et al., 2013a; Durrant et al., 2015). Our data are consistent
 327 with the latter pattern (Figure 3a). For all schema conditions (Schema, No Schema, Incongruent) we
 328 calculated recognition performance as hits minus false alarms (where false alarms pertain to the
 329 new No Schema objects). Participants performed well above chance in all three conditions on both
 330 study-test delays (all $t(23) > 4.9$, $p < 0.0001$). However, there was a significant study-test delay by

331 Schema condition interaction ($F(2,22) = 3.67, p = 0.04$, Wilk's $\Lambda = 0.75$). There was no difference
 332 between schema conditions for recently studied objects (Schema > No schema: $t(23) = -0.93, p =$
 333 0.36 ; Schema > Incongruent: $t(23) = -1.37, p = 0.18$). However, for objects encoded the day before,
 334 participants had better memory for information embedded in a schema quartet than for either
 335 objects encoded in the No schema condition ($t(23) = 2.18, p = 0.04$) or Incongruent quartets
 336 ($t(23) = 2.51, p = 0.02$). Memory did not decline over 24hr for Schema objects ($t(23) = 0.86, p = 0.4$).
 337 In contrast, for No schema ($t(23) = 3.01, p = 0.006$) and Incongruent objects ($t(23) = 3.44, p = 0.002$),
 338 memory was poorer for remote than for recent objects. Response times for hits also decreased as a
 339 result of Study-test delay ($F(1,23) = 23.03, p < 0.001$, Wilk's $\Lambda = 0.50$), but there was no difference
 340 between Schema conditions on this measure. Given this comparison between recent and remote
 341 memories, the schema-benefit that we found on remote memory scores reflected better retention
 342 for schema-based memories (Figure 3b).

343 To investigate whether schema-based memories are less specific and more 'gist-based'
 344 (Winocur et al., 2010), we included similar lures for each target during retrieval, as well as new
 345 objects. Lures consisted of very similar exemplars of the final object of each quartet that had been
 346 presented during encoding (Fig 1b). If memory for objects within a schema is less specific, more false
 347 alarms would occur to the similar lures compared to other novel objects. Indeed, across conditions
 348 there were more false alarms to the similar lures than to new objects. The key finding was that false
 349 alarm rates were highest to the lures of the Schema objects that were encoded just before (Recent
 350 condition: Schema > No schema: $t(23) = 2.02, p = 0.055$; Schema > Incongruent: $t(22) = 2.21, p =$
 351 0.038 ; Figure 3c). However, this pattern of results could also be explained by guesses informed by
 352 prior knowledge (i.e. when not sure about seeing the cowboy's hat, a participant might be more
 353 likely to press "old" because he/she remembered seeing items from a cowboy schema and therefore
 354 saying "old" to the cowboy's hat increases the chance of a hit). Therefore, we also included objects
 355 in the item recognition test that were not seen during encoding, but were congruent with the
 356 schemas used during encoding. We observed that these new 'Schema-related objects' did not elicit

357 more false alarms than the new 'Schema-unrelated objects'. If anything, there was a trend toward
 358 the opposite result (No schema > Schema: $t(23) = 1.92$, $p = 0.067$), with the subjects showing more
 359 correct rejections to the new Schema-related objects than the new Schema-unrelated objects ($t(23)$
 360 $= 2.307$, $p = 0.03$; Figure 3d). This latter finding indicates that the schema is actually beneficial to the
 361 correct identification of new related objects as incorrect lures. To conclude, the supposition that the
 362 schema is used for informed guessing can be ruled out. To the contrary, objects that were
 363 embedded in a schema during encoding have less specific but more resilient memory traces.

364 To summarize, we have shown that shortly after encoding the memory for Schema objects
 365 was already less specific, leading to more false alarms to lures from recently seen Schema objects,
 366 and that this difference between false alarm rates disappeared after a delay of 24 hr. In addition, we
 367 found a behavioral benefit for Schema objects after overnight consolidation. Schema objects showed
 368 no decay in item recognition memory performance, whereas the No schema and Incongruent
 369 objects did display forgetting. We conclude that Schema memories were less specific immediately
 370 after encoding, but were retained better over 24hrs.

371

372 ***fMRI data***

373 *Encoding*

374 The neural correlates of subsequent schema memory

375 The behavioral data demonstrated that after a short delay recognition was at ceiling. The difference
 376 in memory performance between schema conditions became apparent after 24 hr., and was
 377 reflected in better retention of schema embedded objects. Therefore, the analysis of subsequent
 378 memory effects here relates to the delay by schema interaction found in memory performance. To
 379 identify brain regions specifically involved in retention, t-test comparisons were performed
 380 comparing the subject-averaged 'beta-maps' from the schema contrasts between the remote and
 381 recent encoding sessions (using the contrast (remote Schema remembered > remote No schema
 382 remembered) > (recent Schema remembered > no Schema remembered)). We found that the

angular gyrus (AG) showed a Schema > No schema difference that was larger for remote than for recent encoding (Figure 4a, red overlay). For the separate contrast of Schema > Incongruent over time (remote versus recent encoding), we did not find any region at conventionally corrected thresholds (but an uncorrected voxel threshold of 0.005 did point to differential activation in the angular gyrus, hippocampus, superior frontal, and cingulate gyrus).

We plotted the event-related subject-averaged time course and the subject-average beta-weights from the AG region that displayed a larger schema effect with consolidation (Fig 4b and 4c). For all conditions, activation started at a comparable level, but then progressively differed as the schema unfolded. Activation built up monotonically for both the Schema and Incongruent quartets, but this effect was not seen for the No schema quartets. Importantly, activity dropped for the Incongruent condition when the final object no longer fitted the previously built-up schema. Since the AG-region was defined based on the Remote (Schema > No Schema) > Recent (Schema > No schema) contrast, we did not perform inferential statistics comparing the extracted signal across conditions.

To test whether this build-up of a schema is predictive of better performance at retention, we calculated the amount of activity in the schema that was build-up (from the first moment the schema can be inferred at object position 2, up to the final 4th object of the quartet). This measure of schema build-up in the AG in individual participants during encoding correlated with 24 hr. retention measured as Schema hits minus false alarms (the latter pertaining to the New No Schema lures) of those same participants [$r = 0.43$, $p = 0.036$]. This correlation implies that the build-up of schema activity in the AG is beneficial for retaining object memories over 24 hr. This effect was specific to objects encoded in the first, i.e. 'remote encoding session'. In the recent encoding session, there was no schema-build up that was specific for the subsequently remembered objects and no positive correlation between a possible build-up (the difference in activity to object 4 minus object 2) with successful memory retrieval scores [$r = 0.04$, $p = 0.85$]. We also tested whether the activity decrease for the fourth object (response to the fourth object minus response to the third object) in the

Incongruent quartets would be indicative of memory performance (hits minus false alarms to New No Schema objects) as this object might stand out more, similar to an oddball, but we found no evidence for this [$r = -0.8$, $p = 0.71$].

Schema build-up across object sequences

An analytically interesting comparison can be made between the final objects of the Schema and Incongruent quartets that were remembered after 24 hrs. In both cases, these objects were preceded by three objects that belonged to a schema, with only the Incongruent fourth object being out of place. Importantly, this contrast was significant in the angular gyrus (bilaterally) and the right supramarginal gyrus (Fig 4a, green overlay). This means that whereas a host of regions was preferentially activated for a series of schematically congruent versus incongruent objects, only the angular gyrus and supramarginal gyrus were preferentially activated to the fourth object being congruent or incongruent with the preceding object. This finding points to the angular gyrus as the candidate area for holding the schema representation.

The previous analyses already demonstrated (indirectly) a parametric build-up of activity in the AG as successive objects were presented. This build-up is clearly schema-related, as demonstrated by the observed difference between the contrasts for Schema and No schema objects, and between Schema and Incongruent. That is, the initial three objects are modulating AG activity build-up for Schema quartets that contain the subsequently remembered object. Although we had no reason to expect a similar parametric build-up for the No schema condition, a general alteration of activity as a consequence of sequential visual input could not be ruled out. However, our data establish that the AG is not a candidate area for such a general effect, but there might be other regions that do show either a parametric build-up or even a parametric decline. Therefore, we also performed whole-brain analyses to identify regions where activity was modulated by a parametric regressor in either encoding session, for quartets that contained subsequently remembered objects. The parametric regressor represented the hypothesized build-up or decline of activation with each

435 successive presentation of an object in the quartet containing the remembered final object. We
 436 tested for activity that fitted the parametric regressor for the quartets containing the subsequently
 437 remembered final objects. An overview of all brain regions is presented in Table 1. In the remote
 438 encoding session, the remembered No schema quartets did not elicit reliable parametric variation in
 439 brain activity in any region, whereas the remembered Incongruent quartets showed a parametric
 440 increase in the left superior frontal gyrus and a decrease in the right angular gyrus. As expected,
 441 during the remote encoding session, activity for the schema quartets that contained the
 442 subsequently remembered objects was parametrically modulated in the angular gyrus, confirming
 443 the analyses presented above. A particularly interesting observation was a parametric decrease for
 444 the remembered Schema quartets in the hippocampus (Fig. 5a, blue overlay), suggestive of a
 445 disengagement of the hippocampus when encoding schema memories.

446 For the recent encoding session, we found no parametric modulation of activity in
 447 subsequently remembered Schema quartets. When taking remembered and forgotten schema
 448 quartets together, the left angular gyrus did show a parametric increase in activity (peak: $x = -45$, $y =$
 449 -64 , $z = 22$ $t(23) = 3.99$, $p < 0.001$). This shows that for recently encoded objects the schema is being
 450 build-up in the angular gyrus as well, but that this build-up is apparently only beneficial for
 451 remembering these objects after a period of 24 hr. This is consistent with the build-up being
 452 associated with consolidation. We also found no parametric schema effect for subsequently
 453 remembered quartets (Schema parametric > No schema parametric). During remote encoding we
 454 found a parametric schema effect in areas that largely overlapped with the main effect of schema
 455 (see Fig 4a blue overlay and Table 2) including the AG.

456 Since the AG is being modulated by the build-up of a schema by presenting related objects,
 457 we suspected that the object representations in the ventral visual stream could be contributing to
 458 the schema build-up. A connectivity analysis (PPI) using the lateral occipital region from the localizer
 459 scan (objects > scrambled) as seed did indeed show that this region was connected to the AG during

460 encoding of schema objects, (see fig 4a orange overlay). This AG area overlaps almost completely
 461 with the AG regions showing a remote schema effect and schema build-up.

462

463 Interplay between AG and hippocampus during encoding of schema quartets

464 The parametric decrease that we observed in the hippocampus (Fig 5b) raises the intriguing
 465 possibility that the connection between the AG and hippocampus is inhibitory in nature and leads to
 466 the hippocampus becoming less involved in encoding memories when a schema is present. This fits
 467 with a model of accelerated systems-level consolidation for schema memories. Interestingly, the
 468 parametric value for the Schema decrease in the posterior hippocampus correlated negatively with
 469 the amount of schema build-up in AG (Fig 5c, $r = -0.45$, $p = 0.027$). This indicates that a greater
 470 schema build-up effect was paired with a stronger parametric decrease of activity in the
 471 hippocampus. This could mean that the AG, as it is becoming more involved in encoding Schema
 472 objects, starts signaling the hippocampus that its involvement is no longer necessary. To test this
 473 idea, we performed a PPI connectivity analysis with the same AG seed region, investigating increased
 474 connectivity as a function of the parametric build-up of a schema. This analysis revealed that the
 475 right posterior hippocampus is indeed functionally coupled to the AG during encoding and that the
 476 degree of connectivity is modulated in association with the parametric build-up of the schema
 477 during presentation of the quartets (Fig 5a, red overlay).

478 The differential expression of detailed versus gist-like memory representations may reflect
 479 differential activation in hippocampus and cortex. Specifically, if the hippocampus disengages, there
 480 may be a less detailed memory trace. We therefore examined the correlation between false alarms
 481 and AG-hippocampus PPI connectivity scores. Those participants with higher AG-hippocampus PPI
 482 connectivity did not show more false alarms to Schema lures ($r = 0.07$, $p = \text{ns}$), but they did show a
 483 higher rate of false alarms to new Schema objects ($r = 0.48$, $p = 0.018$). The higher number of false
 484 alarms to new objects from the same schema may indicate that when detailed memory of the

485 schema objects is lacking, because of less hippocampal involvement during encoding, the gist of the
 486 schema prevails.

487

488 *Retrieval*

489 Interaction between schema condition and study-test delay in medial prefrontal cortex (mPFC) at
 490 retrieval.

491 It was of interest to explore whether the neuronal schema effect during retrieval mirrors the schema
 492 effect found during encoding and in the behavioral data, in the sense that they become apparent
 493 only after consolidation. An interaction between Schema condition and Study-test delay was
 494 observed in the medial prefrontal cortex during retrieval (mPFC, coordinates of the peak: $x = -6$, $y =$
 495 39 , $z = 2$, $F(1,23) = 26$, $p < 0.05$ Small Volume Corr.; Figure 6). To secure insight into the direction of
 496 this interaction, we extracted beta-weights from the mPFC for remote and recent hits in each
 497 condition. When comparing these subject-averaged beta-weights, we found that mPFC activity was
 498 higher for Schema than No schema for remote hits ($t=2.54$, $p = 0.011$) and Schema activation was
 499 also higher for remote than recent Schema hits ($t=2.33$, $p = 0.020$). However, Incongruent hits did
 500 not differ from either Schema (remote: $t = 1.39$, $p = 0.16$) and No schema hits (remote: $t = 1.09$, $p =$
 501 0.27). MPFC activity to Incongruent hits showed a trend towards increased activity over time
 502 (Incongruent: remote > recent: $t=1.87$, $p = 0.06$). This interaction confirmed that the schema
 503 differences in mPFC become apparent after a 24 h delay at the same time as the behavioral benefit
 504 arises.

505

506 Schema effect in parietal cortex

507 To test whether there were brain areas that were more activated by Schema relative to No schema
 508 during item recognition, we used a direct contrast between conditions (omitting the misses). We
 509 found five areas that responded more to Schema than No schema, these were the right AG, left
 510 parahippocampal gyrus, left precuneus (extending into the cuneus), the dorsal medial thalamic

nucleus, and left inferior parietal lobe (Figure 6). No areas were more active during retrieval of No schema or Incongruent objects than Schema objects. Since the AG showed behaviorally relevant schema activation during encoding, the AG and parietal areas were further inspected in an ROI analysis (Figure 7). Using a PPI analysis with remote Schema memories versus remote No schema memories (hits) we found connectivity with the AG to be higher for the remote Schema memories in several areas in the left hemisphere (Figure 8). Furthermore, we found increased connectivity between AG and LOC that correlated positively with correct recognition (proportion hits) of remote Schema objects ($r = 0.42$, $p = 0.039$). To rule out a general effect of retrieval success we also calculated the correlation between the PPI value in the AG and hits to No schema objects and there we found no correlation ($r = -0.18$, $p = \text{ns}$) and the difference between both correlations was significant ($Z = 2.08$, $p = 0.038$). These findings suggest that the AG is specifically involved in successful retrieval of schema objects.

Discussion

Schemas are believed to be beneficial for memory of conceptually related information (Bransford and Johnson, 1972) and thought to accelerate consolidation (Wang and Morris, 2010; van Kesteren et al., 2012; Ghosh and Gilboa, 2014). Here we found behavioral and neuroimaging evidence for accelerated consolidation for schema memories that could be linked to memory processes in the angular gyrus (AG), hippocampus, and medial prefrontal cortex (mPFC) during encoding, consolidation and retrieval.

First, objects embedded in a schema (that our subjects identified as successive stimuli were presented) were better remembered 24hr later compared to those that were either not embedded in a schema or incongruent with one. Second, during encoding, the AG showed an activity pattern that reflected the build-up of a schema. This build-up of activity was specific for schema memories that were retained for 24hr, with the amount of AG build-up predictive of memory retention. One interesting aspect of 'build-up' is that it parallels old data from Bransford (Bransford, 1979; Morris et

al., 1979), which suggests schemas are only effective as aids to memory if they are activated. This was first shown in Bransford's famous story about 'washing clothes', a schema which everyone has presumably obtained, but which in the story was obscured by the manner in which the passage of prose was written. Once the theme was revealed, its effectiveness for supporting memory is dramatic. Third, in parallel with the build-up in AG, we observed that the hippocampus decreased its activity when a schema was presented. Disengagement of the hippocampus from encoding a schema object fits with the notion that schemas are stored in the neocortex and accelerate systems-level consolidation (Tse et al., 2007; Tse et al., 2008; van Kesteren et al., 2010a). It also provides a potential explanation why schema memories were found to be less specific, or less detailed, compared to memories that were not embedded in a schema.

There are subtle features of the behavioral data related to the specificity of memory. For example, the behavioral schema effect (positive difference in memory scores between schema and no-schema conditions) was not present immediately after encoding, but emerged after consolidation. This fits with previous reports of a benefit for schema memories after a night of sleep (Tse et al., 2007; van Kesteren et al., 2013a; Durrant et al., 2015). Comparing remote and recent schema memories within participants enabled us to conclude that the schema effect reflects better retention across time for schema objects, indicating that a schema makes memories more resilient to forgetting. However, such a result could also be explained by using a schema for informed guessing after a delay and we sought data that might help to distinguish between a consolidation and guessing interpretation. Overall, for schema and non-schema conditions, participants made more false alarms and less correct rejections to the lures that were similar to the targets relative to new lures. This has also been reported in other studies (Gutchess and Schacter, 2012; Bowman and Dennis, 2015). However, we also observed that our participants made more false alarms to similar lures of targets that might potentially have been embedded in a schema during encoding relative to lures from both non-schema conditions. This subtle detail indicates that schema memories can be less detailed and possibly more gist-based. However, the critical comparison to rule out guessing

563 was whether the participants would falsely recognize new objects that were related to the schema
564 but not seen during encoding; that is, they were first encountered during item recognition. It turns
565 out they did *not* make more false alarms to these new schema lures compared to new no-schema
566 lures. In fact, they made more correct rejections to the new schema lures. These findings together
567 suggest that schemas are not used for guessing, but that objects related to a schema are encoded in
568 a less specific manner, thereby giving rise to more false alarms directly after encoding.

569 Might the finding of less specificity for memories of schema objects be related to the
570 reduced involvement of the hippocampus in memorizing objects from a schema? The hippocampus
571 has circuitry well-suited for discriminating between studied items and similar lures, and does so
572 through pattern-separation (Bakker et al., 2008; Yassa and Stark, 2011). In our study, we found that
573 targets and similar lures from a schema were more difficult to dissociate. One possibility is that a
574 schema could act, in part, as an inhibitor of hippocampal functioning, as proposed by the SLIMM
575 framework (van Kesteren et al., 2012). In our experiment, the AG showed functional coupling with
576 the posterior hippocampus. More schema-related activity in AG was associated with greater
577 deactivation of the hippocampus. In addition, a larger influence of AG on hippocampus was related
578 to more false alarms to new schema objects, indicative that the gist but not the details of the
579 memory were preserved. Overall, the finding of less hippocampal involvement for schema memories
580 fits with the findings from rodents (Tse et al., 2007; Tse et al., 2008) and humans (van Kesteren et al.,
581 2010a; van Kesteren et al., 2014) and provides more evidence for accelerated consolidation of
582 schema memories. In addition, it provides an explanation why schema memories seem less detailed
583 and more gist-based (Lewis and Durrant, 2011).

584 What is the relative role of mPFC and AG? To date, the partial disengagement of the MTL
585 memory system for schema-memories has been linked to the allocation of the neural correlates of
586 schema memory to the medial prefrontal cortex (mPFC) – during both encoding (van Kesteren et al.,
587 2010a; van Kesteren et al., 2012; van Kesteren et al., 2013b; van Kesteren et al., 2014) and retrieval
588 (van Kesteren et al., 2010b; Brod et al., 2015). We found no evidence for involvement of the mPFC

during encoding of objects embedded in a schema, but the mPFC did show an interaction between study-test delay and schema condition when monitored at the time of retrieval. This result confirms extensive data pointing to the involvement of the mPFC in retrieving remote memories (Bontempi et al., 1999; Frankland et al., 2004; Maviel et al., 2004; Takashima et al., 2006; Takehara-Nishiuchi et al., 2006; Gais et al., 2007; Takehara-Nishiuchi and McNaughton, 2008; Takashima et al., 2009; Goshen et al., 2011; Bonnici et al., 2012). In contrast, the retention of schema objects for 24hr was related to a build-up of schema activity in the AG during encoding. The AG is high-up in the hierarchy of convergence for unimodal and supramodal representations (Fernandino et al., 2015), which fits with the content of a schema. In addition, the AG is involved in processing thematic relationships (Kalenine et al., 2009), closely resembling the kind of schemas used in our experiment. This also fits with the notion that the AG is a 'binding zone' that is believed to combine representations in a conceptual manner (Binder et al., 2009a; Binder and Desai, 2011; Shimamura, 2011; Price et al., 2015). This binding function of the AG has recently been linked directly to recombining visual representations into schemas (Wagner et al., 2015), in accordance with our findings.

Connectivity analyses using PPI revealed that object representations in LOC seemed to co-activate along with the related schema in AG. Typically, response patterns in LOC elicited by pictures of objects show categorical clustering (Eger et al., 2008). This clustering is remarkably consistent across species (Kriegeskorte et al., 2008) and reflects categorical as well as shape similarity (Bracci and Op de Beeck, 2016). It is likely that the AG receives 'bottom-up' information when object representations are activated that show conceptual clustering. The AG then binds these related representations in a schema during encoding. During retrieval, the AG responded more to those objects that were embedded in a schema during encoding compared to non-schema objects. This likely reflects that the schema was also active during retrieval. Such retrieval-associated AG activation of a schema (consisting of related and connected object representations) leads to the expectation that the AG would similarly be connected to ventral visual representation areas such as LOC during item recognition. The successful linking of the schema to these object representations

would be beneficial to memory scores, as was observed. In addition, connectivity from AG to visual representation area such as the LOC, overlapping with those found in our object localizer, was higher for remote schema memories than for remote No schema memories. This finding corroborates a recent study in which it was also shown that the interplay between AG and ventral visual areas was important for memory success (Kuhl and Chun, 2014). Thus, during retrieval, schema information is used to reactivate object representations in LOC and to match the target to the previously seen object representations.

To conclude, this study provides behavioral and neuronal evidence to support the idea that schemas give rise to improved memory consolidation. The mPFC is involved in the retrieval of memories dependent on schemas. However, at least for the type of task described here, the schema information itself appears to be stored in the AG. Schema activation in AG at encoding determines whether an object is successfully remembered after 24hr. The AG binds together schema-related object representations during encoding and uses this information again during retrieval. The simultaneous disengagement of the hippocampus from schema memory formation is further evidence for accelerated schema-associated consolidation and provides a potential explanation of why schema memories are less detailed.

Author contributions

Conceptualization, M.vdL., R.B., R.M., and G.F.; Investigation, M.vdL.; Writing – Original Draft, M.vdL.; Writing – Review & Editing, M.vdL., R.B., R.M., and G.F.; Funding Acquisition, G.F. and R.M.

639 **References (current style = Harvard)**

- 640 Alvarez P, Squire LR (1994) Memory consolidation and the medial temporal lobe: a simple network
641 model. *Proc Natl Acad Sci U S A* 91:7041-7045.
- 642 Bakker A, Kirwan CB, Miller M, Stark CE (2008) Pattern separation in the human hippocampal CA3
643 and dentate gyrus. *Science* 319:1640-1642.
- 644 Binder JR, Desai RH (2011) The neurobiology of semantic memory. *Trends in Cognitive Sciences*
645 15:527-536.
- 646 Binder JR, Desai RH, Graves WW, Conant LL (2009a) Where Is the Semantic System? A Critical Review
647 and Meta-Analysis of 120 Functional Neuroimaging Studies. *Cerebral Cortex* 19:2767-2796.
- 648 Binder JR, Desai RH, Graves WW, Conant LL (2009b) Where is the semantic system? A critical review
649 and meta-analysis of 120 functional neuroimaging studies. *Cereb Cortex* 19:2767-2796.
- 650 Bonnici HM, Chadwick MJ, Lutti A, Hassabis D, Weiskopf N, Maguire EA (2012) Detecting
651 representations of recent and remote autobiographical memories in vmPFC and
652 hippocampus. *J Neurosci* 32:16982-16991.
- 653 Bontempi B, Laurent-Demir C, Destrade C, Jaffard R (1999) Time-dependent reorganization of brain
654 circuitry underlying long-term memory storage. *Nature* 400:671-675.
- 655 Bowman CR, Dennis NA (2015) The neural correlates of correctly rejecting lures during memory
656 retrieval: the role of item relatedness. *Exp Brain Res* 233:1963-1975.
- 657 Boynton GM, Engel SA, Glover GH, Heeger DJ (1996) Linear systems analysis of functional magnetic
658 resonance imaging in human V1. *Journal of Neuroscience* 16:4207-4221.
- 659 Bracci S, Op de Beeck HP (2016) Dissociations and associations between shape and category
660 representations in the two visual pathways. *The Journal of Neuroscience*.
- 661 Bransford J (1979) The role of prior knowledge. *Human Cognition: Learning, Understanding and*
662 *Remembering Conceptual Processes*.
- 663 Bransford JD, Johnson MK (1972) Contextual Prerequisites for Understanding - Some Investigations
664 of Comprehension and Recall. *J Verb Learn Verb Be* 11:717-726.
- 665 Brod G, Lindenberger U, Werkle-Bergner M, Shing YL (2015) Differences in the neural signature of
666 remembering schema-congruent and schema-incongruent events. *Neuroimage* 117:358-366.
- 667 Danker JF, Anderson JR (2010) The ghosts of brain states past: remembering reactivates the brain
668 regions engaged during encoding. *Psychol Bull* 136:87-102.
- 669 Durrant SJ, Cairney SA, McDermott C, Lewis PA (2015) Schema-conformant memories are
670 preferentially consolidated during REM sleep. *Neurobiol Learn Mem* 122:41-50.
- 671 Eger E, Ashburner J, Haynes JD, Dolan RJ, Rees G (2008) fMRI activity patterns in human LOC carry
672 information about object exemplars within category. *J Cogn Neurosci* 20:356-370.
- 673 Fernandino L, Binder JR, Desai RH, Pendl SL, Humphries CJ, Gross WL, Conant LL, Seidenberg MS
674 (2015) Concept Representation Reflects Multimodal Abstraction: A Framework for Embodied
675 Semantics. *Cereb Cortex*.
- 676 Frankland PW, Bontempi B (2005) The organization of recent and remote memories. *Nat Rev*
677 *Neurosci* 6:119-130.
- 678 Frankland PW, Bontempi B, Talton LE, Kaczmarek L, Silva AJ (2004) The involvement of the anterior
679 cingulate cortex in remote contextual fear memory. *Science* 304:881-883.
- 680 Friston KJ, Buechel C, Fink GR, Morris J, Rolls E, Dolan RJ (1997) Psychophysiological and modulatory
681 interactions in neuroimaging. *Neuroimage* 6:218-229.
- 682 Gais S, Albouy G, Boly M, Dang-Vu TT, Darsaud A, Desseilles M, Rauchs G, Schabus M, Sterpenich V,
683 Vandewalle G, Maquet P, Peigneux P (2007) Sleep transforms the cerebral trace of
684 declarative memories. *Proc Natl Acad Sci U S A* 104:18778-18783.
- 685 Ghosh VE, Gilboa A (2014) What is a memory schema? A historical perspective on current
686 neuroscience literature. *Neuropsychologia* 53:104-114.
- 687 Goshen I, Brodsky M, Prakash R, Wallace J, Gradinaru V, Ramakrishnan C, Deisseroth K (2011)
688 Dynamics of retrieval strategies for remote memories. *Cell* 147:678-689.

- 689 Gutchess AH, Schacter DL (2012) The neural correlates of gist-based true and false recognition.
690 Neuroimage 59:3418-3426.
- 691 Hanson SJ, Hanson C, Halchenko Y, Matsuka T, Zaimi A (2007) Bottom-up and top-down brain
692 functional connectivity underlying comprehension of everyday visual action. Brain Struct
693 Funct 212:231-244.
- 694 Kalenine S, Peyrin C, Pichat C, Segebarth C, Bonthoux F, Baciú M (2009) The sensory-motor specificity
695 of taxonomic and thematic conceptual relations: a behavioral and fMRI study. Neuroimage
696 44:1152-1162.
- 697 Kriegeskorte N, Mur M, Ruff DA, Kiani R, Bodurka J, Esteky H, Tanaka K, Bandettini PA (2008)
698 Matching categorical object representations in inferior temporal cortex of man and monkey.
699 Neuron 60:1126-1141.
- 700 Kuhl BA, Chun MM (2014) Successful remembering elicits event-specific activity patterns in lateral
701 parietal cortex. J Neurosci 34:8051-8060.
- 702 Lee IA, Preacher KJ (2013) Calculation for the test of the difference between two dependent
703 correlations with no variable in common. Available from <http://quantpsy.org>. In.
- 704 Lewis PA, Durrant SJ (2011) Overlapping memory replay during sleep builds cognitive schemata.
705 Trends Cogn Sci 15:343-351.
- 706 Malach R, Reppas JB, Benson RR, Kwong KK, Jiang H, Kennedy WA, Ledden PJ, Brady TJ, Rosen BR,
707 Tootell RB (1995) Object-related activity revealed by functional magnetic resonance imaging
708 in human occipital cortex. Proc Natl Acad Sci U S A 92:8135-8139.
- 709 Maviel T, Durkin TP, Menzaghi F, Bontempi B (2004) Sites of neocortical reorganization critical for
710 remote spatial memory. Science 305:96-99.
- 711 Morris CD, Stein BS, Bransford JD (1979) Prerequisites for the Utilization of Knowledge in the Recall
712 of Prose Passages. J Exp Psychol-Hum L 5:253-261.
- 713 Nyberg L, Habib R, McIntosh AR, Tulving E (2000) Reactivation of encoding-related brain activity
714 during memory retrieval. Proc Natl Acad Sci U S A 97:11120-11124.
- 715 Price AR, Bonner MF, Peelle JE, Grossman M (2015) Converging evidence for the neuroanatomic
716 basis of combinatorial semantics in the angular gyrus. J Neurosci 35:3276-3284.
- 717 Scoville WB, Milner B (1957) Loss of recent memory after bilateral hippocampal lesions. J Neurol
718 Neurosurg Psychiatry 20:11-21.
- 719 Shimamura AP (2011) Episodic retrieval and the cortical binding of relational activity. Cogn Affect
720 Behav Neurosci 11:277-291.
- 721 Squire LR (1986) Mechanisms of memory. Science 232:1612-1619.
- 722 Sweegers CC, Takashima A, Fernandez G, Talamini LM (2014) Neural mechanisms supporting the
723 extraction of general knowledge across episodic memories. Neuroimage 87:138-146.
- 724 Takashima A, Nieuwenhuis IL, Jensen O, Talamini LM, Rijpkema M, Fernandez G (2009) Shift from
725 hippocampal to neocortical centered retrieval network with consolidation. J Neurosci
726 29:10087-10093.
- 727 Takashima A, Petersson KM, Rutters F, Tendolkar I, Jensen O, Zwarts MJ, McNaughton BL, Fernandez
728 G (2006) Declarative memory consolidation in humans: a prospective functional magnetic
729 resonance imaging study. Proc Natl Acad Sci U S A 103:756-761.
- 730 Takehara-Nishiuchi K, McNaughton BL (2008) Spontaneous changes of neocortical code for
731 associative memory during consolidation. Science 322:960-963.
- 732 Takehara-Nishiuchi K, Nakao K, Kawahara S, Matsuki N, Kirino Y (2006) Systems consolidation
733 requires postlearning activation of NMDA receptors in the medial prefrontal cortex in trace
734 eyeblink conditioning. J Neurosci 26:5049-5058.
- 735 Talairach J, Tournoux P (1988) Co-planar stereotaxic atlas of the human brain : 3-dimensional
736 proportional system : an approach to medical cerebral imaging. New York: Thieme Medical
737 Publishers.

- 738 Tse D, Langston RF, Bethus I, Wood ER, Witter MP, Morris RG (2008) Does assimilation into schemas
739 involve systems or cellular consolidation? It's not just time. *Neurobiol Learn Mem* 89:361-
740 365.
- 741 Tse D, Langston RF, Kakeyama M, Bethus I, Spooner PA, Wood ER, Witter MP, Morris RG (2007)
742 Schemas and memory consolidation. *Science* 316:76-82.
- 743 Tse D, Takeuchi T, Kakeyama M, Kajii Y, Okuno H, Tohyama C, Bito H, Morris RG (2011) Schema-
744 dependent gene activation and memory encoding in neocortex. *Science* 333:891-895.
- 745 Tulving E, Thomson DM (1973) Encoding Specificity and Retrieval Processes in Episodic Memory.
746 *Psychol Rev* 80:352-373.
- 747 van Buuren M, Kroes MC, Wagner IC, Genzel L, Morris RG, Fernandez G (2014) Initial investigation of
748 the effects of an experimentally learned schema on spatial associative memory in humans. *J*
749 *Neurosci* 34:16662-16670.
- 750 van Kesteren MT, Fernandez G, Norris DG, Hermans EJ (2010a) Persistent schema-dependent
751 hippocampal-neocortical connectivity during memory encoding and postencoding rest in
752 humans. *Proc Natl Acad Sci U S A* 107:7550-7555.
- 753 van Kesteren MT, Rijpkema M, Ruiter DJ, Fernandez G (2010b) Retrieval of associative information
754 congruent with prior knowledge is related to increased medial prefrontal activity and
755 connectivity. *J Neurosci* 30:15888-15894.
- 756 van Kesteren MT, Ruiter DJ, Fernandez G, Henson RN (2012) How schema and novelty augment
757 memory formation. *Trends in Neuroscience* 35:211-219.
- 758 van Kesteren MT, Rijpkema M, Ruiter DJ, Fernandez G (2013a) Consolidation differentially modulates
759 schema effects on memory for items and associations. *PLoS ONE* 8:e56155.
- 760 van Kesteren MT, Rijpkema M, Ruiter DJ, Morris RG, Fernandez G (2014) Building on prior knowledge:
761 schema-dependent encoding processes relate to academic performance. *J Cogn Neurosci*
762 26:2250-2261.
- 763 van Kesteren MT, Beul SF, Takashima A, Henson RN, Ruiter DJ, Fernandez G (2013b) Differential roles
764 for medial prefrontal and medial temporal cortices in schema-dependent encoding: from
765 congruent to incongruent. *Neuropsychologia* 51:2352-2359.
- 766 Wagner IC, van Buuren M, Kroes MC, Gutteling TP, van der Linden M, Morris RG, Fernandez G (2015)
767 Schematic memory components converge within angular gyrus during retrieval. *Elife* 4.
- 768 Wang SH, Morris RG (2010) Hippocampal-neocortical interactions in memory formation,
769 consolidation, and reconsolidation. *Annu Rev Psychol* 61:49-79, C41-44.
- 770 Winocur G, Moscovitch M, Bontempi B (2010) Memory formation and long-term retention in
771 humans and animals: convergence towards a transformation account of hippocampal-
772 neocortical interactions. *Neuropsychologia* 48:2339-2356.
- 773 Yassa MA, Stark CEL (2011) Pattern separation in the hippocampus. *Trends in neurosciences* 34:515-
774 525.

775

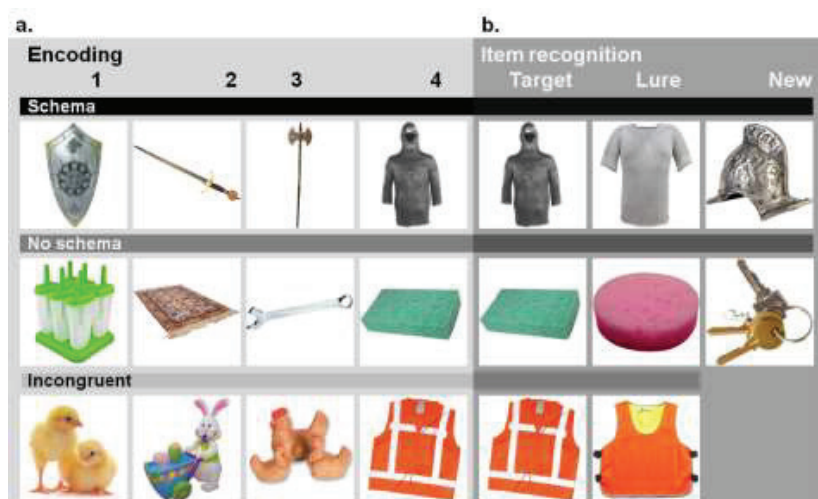
776

777

778

779 **Figures and legend**

780 **Figure 1**



781

782 **Fig 1. Stimuli. a.** During both encoding sessions, participants were presented with quartets

783 belonging to the Schema, No schema, and Incongruent conditions. A quartet consisted of four

784 objects that were presented serially. The first quartet (row 1) is an example of the “knight” schema.

785 Next, in the No schema condition (row 2), four objects that have no pre-existing association were

786 presented. For the Incongruent condition (row 3), the first three objects from the “Easter” schema

787 were followed by an incongruent final object (e.g. a high-visibility vest). **b.** During item recognition,

788 the participants were presented with the quartets’ final objects (column 1). The quartet’s final object

789 was presented once exactly as seen before (Target) and once as a very similar exemplar of the same

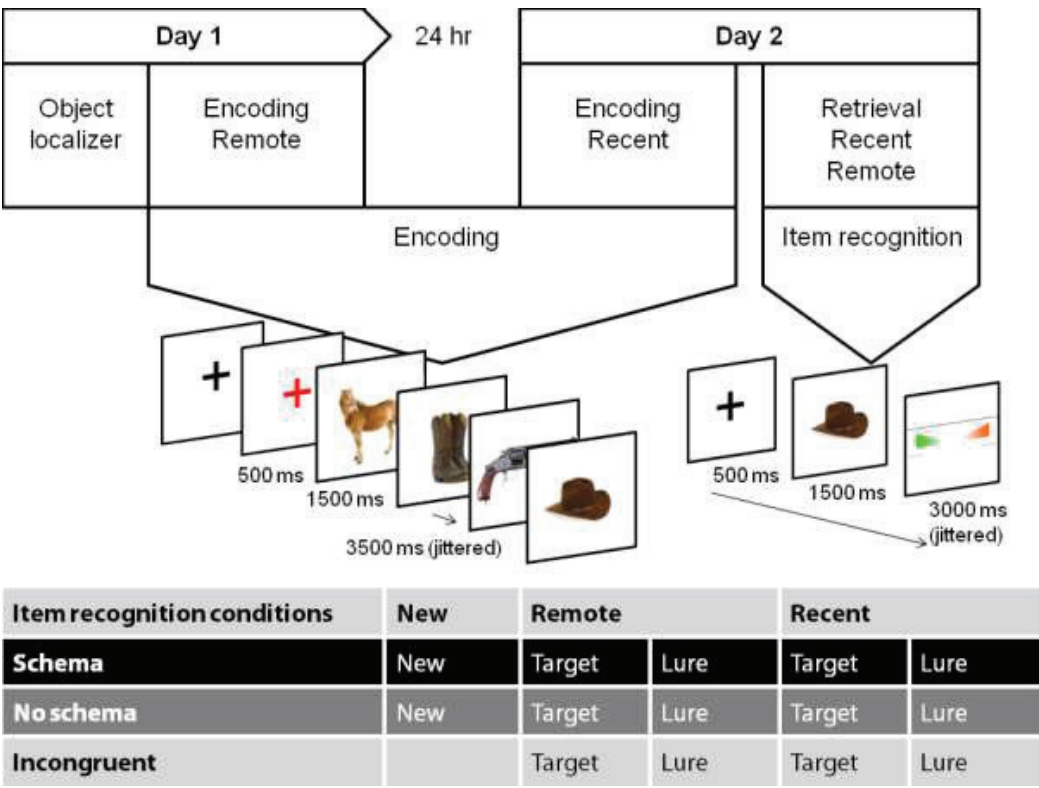
790 object (Lure; column 2). In addition (column 3), there were objects that were new and belonged to

791 the schemas that were presented (new Schema-related) or new but unrelated objects (new Schema-

792 unrelated).

793

794 **Figure 2.**



796 **Fig 2. Design. a.** Participants were scanned on two consecutive days. On the first day, they encoded
 797 the first set of objects (remote condition). After 24 hr. they returned to the lab to encode the second
 798 set of objects (recent condition). The second encoding session was followed by the item recognition
 799 task after a short break. **b.** During encoding four objects were presented serially (for 1500 ms each).
 800 Participants were instructed to memorize the objects and quartets and to indicate for each object
 801 whether it fitted in a shoebox ("yes" or "no"). A black fixation cross was visible on screen throughout
 802 the experiment and this fixation-cross changed to red to signal the start of a new quartet. The inter-
 803 stimulus interval was 3.5 s on average. All inter-stimulus intervals were jittered between 1.5 and 5.5
 804 s. During item recognition the participants were presented with pictures of objects (1500 ms). They
 805 rated their memory for the objects using a 6-level confidence scale, ranging from 1 (very surely old)
 806 to 6 (very surely new). After a jittered interval (average = 3.5 s, range: 1.5 – 4.5 s), during which the

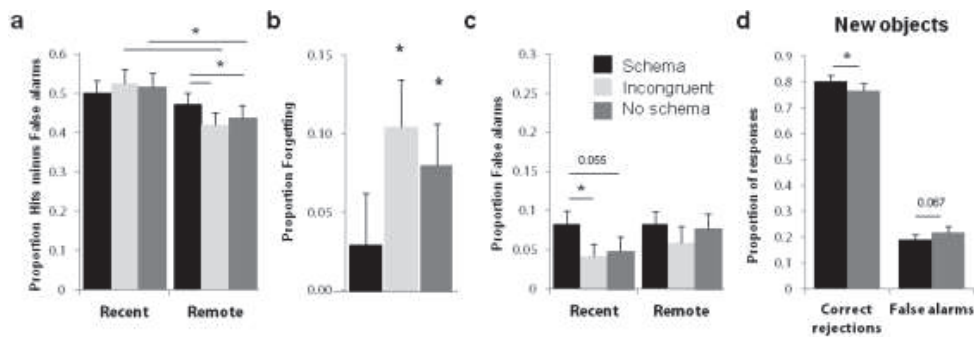
807 confidence levels were displayed on screen, the next object was presented. c. Objects were
808 presented during item recognition across 14 conditions, with 700 objects distributed equally over
809 Schema condition (Schema, No schema, and Incongruent), Study-test delay (New, Remote, and
810 Recent), and Type of object (Target or Lure), resulting in 50 objects per bin.

811

812

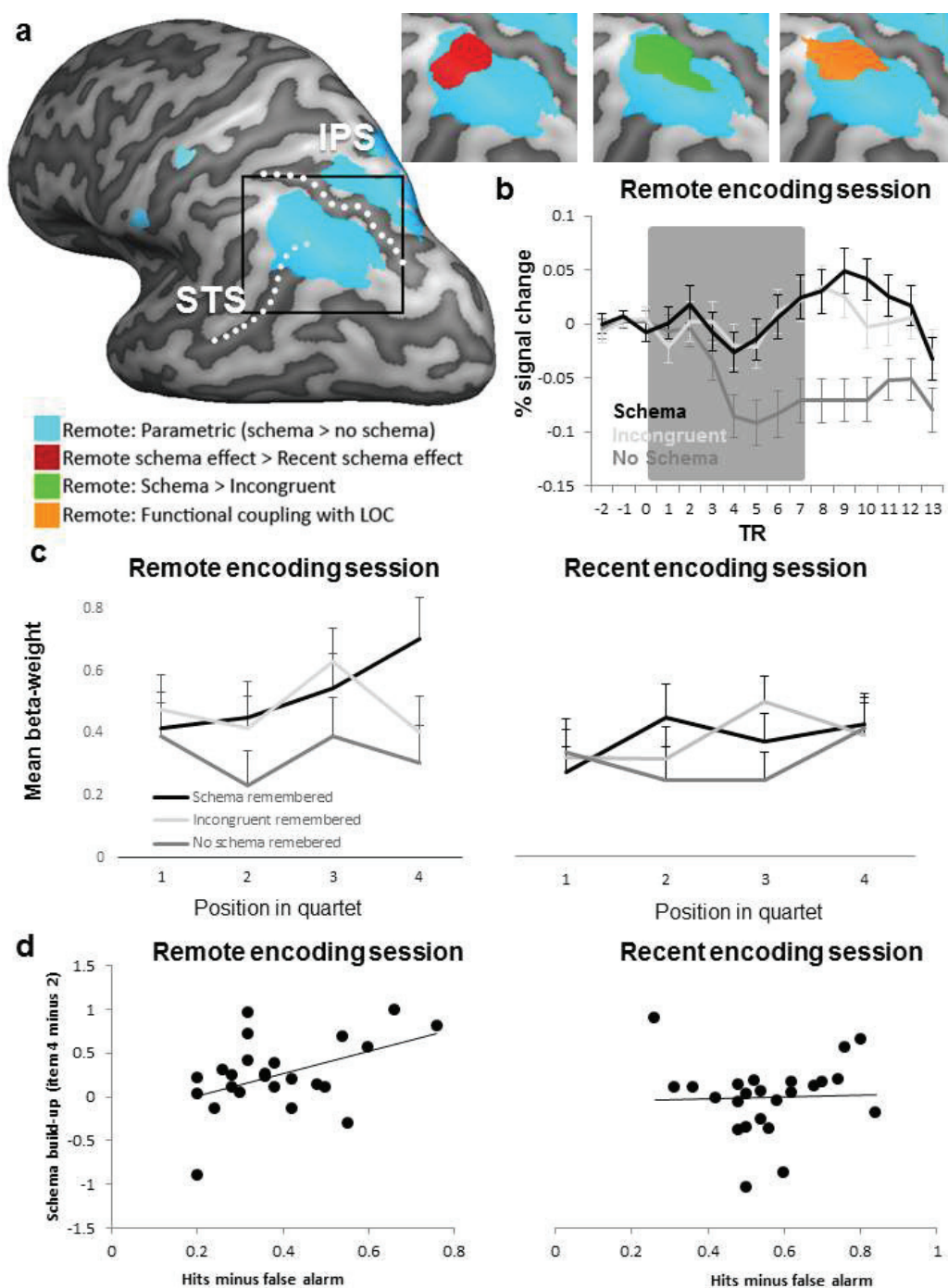
813

814 **Figure 3.**



816 **Fig 3. Behavioral data.** **a.** Proportion of hits (hits minus false alarms to the new No schema condition)
 817 are presented for recent and remote conditions for Schema, Incongruent and No Schema conditions.
 818 **b.** Proportion of forgetting (recent minus remote hits) is presented for the three schema conditions.
 819 **c.** Proportion of false alarms for all schema conditions (false alarms minus the proportion of false
 820 alarms to the new No schema condition) are presented for recent and remote conditions. **d.**
 821 Proportion of correct rejections and false alarms to the new No schema and new Schema objects are
 822 presented. For all plots: black color represents the Schema condition, dark gray: Incongruent, and
 823 light gray: No schema. Error bars represent the standard error of the mean (S.E.M.). * denotes a
 824 significant p -value of < 0.05 .

827 Figure 4.



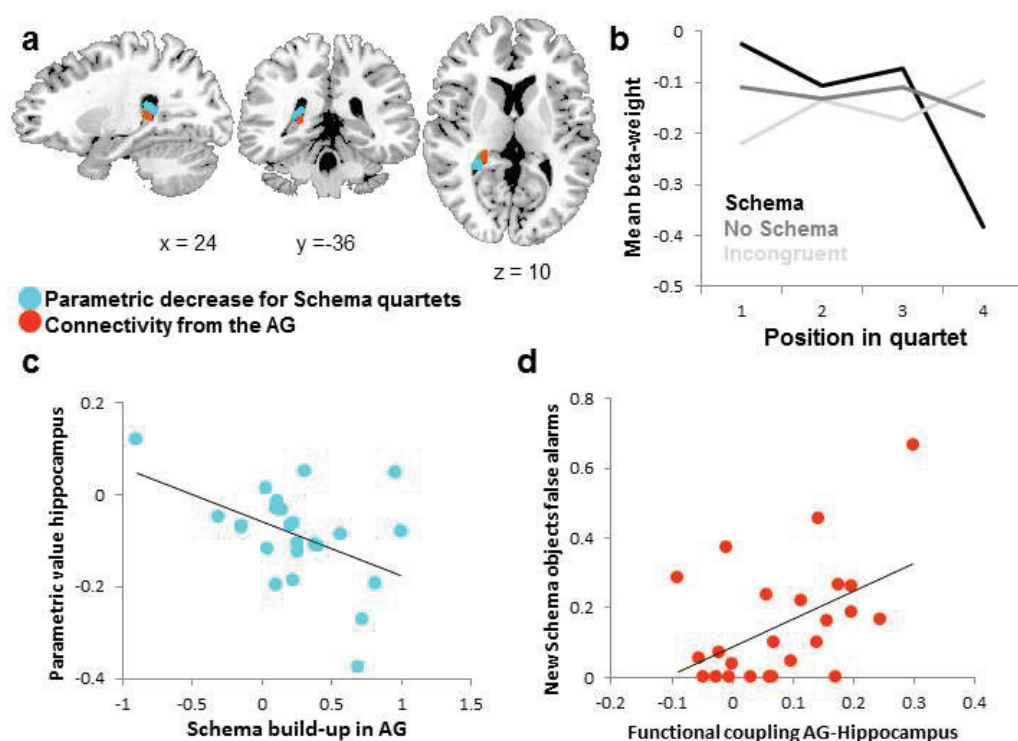
828

829 Figure 4. Schema effects in the AG during encoding. a. Inflated hemisphere (left hemisphere, dark

830 gray areas are sulci) with overlays of four contrasts that all converge in the angular gyrus. In green,

831 areas that were more active in the remote encoding session to Schema than to Incongruent
 832 remembered final objects. In orange, areas that showed functional coupling with the LOC during
 833 encoding of subsequently remembered Schema objects. In red areas that showed a larger schema
 834 effect in the remote encoding session as compared to the recent encoding session ((remote Schema
 835 remembered > remote No schema remembered) > (recent Schema remembered > no Schema
 836 remembered)). In blue, areas that showed a parametric schema effect, i.e. a build up of activation
 837 with each object presentation (parametrically modulated activity during schema quartets >
 838 parametrically modulated activity during No schema quartets). The dotted lines present the superior
 839 temporal sulcus (STS) and intraparietal sulcus (IPS) and are depicted for anatomical reference. All
 840 maps were corrected at a cluster-level of $p < 0.05$ (voxel-level threshold was $p < 0.001$). **b.** The
 841 subject-averaged event-related time course from the AG region defined by the contrast: remote
 842 (Schema > No schema) > recent (Schema > No schema) and is presented by the red blob in Fig. 4a.
 843 We plotted the percent signal change at each TR (TR was 2190ms) for the three schema conditions
 844 (black: Schema, light gray: Incongruent, dark gray: No schema). The gray area indicates the time of
 845 the presentation of the quartet, the first object is presented at TR= 0 and the offset of the final
 846 object of the quartet is on average (with jittered intervals) at TR= 7. Error bars are S.E.M. **c.** For each
 847 encoding session, we plotted the subject-averaged beta-weight for each of the four objects in the
 848 quartet from the same ROI as used in Fig. 4b. In black for schema quartets, in light gray incongruent
 849 quartets and in dark gray No schema quartets. **d.** The correlation between the build-up of a schema
 850 (beta-weight to object 4 minus beta-weight to object 2) and the proportion of hits minus false
 851 alarms is plotted for both encoding sessions (from the same ROI as used in Fig. 4b). Remote
 852 encoding session is the session that was 24 hr. prior to retrieval. Recent encoding session was the
 853 session immediately preceding retrieval.

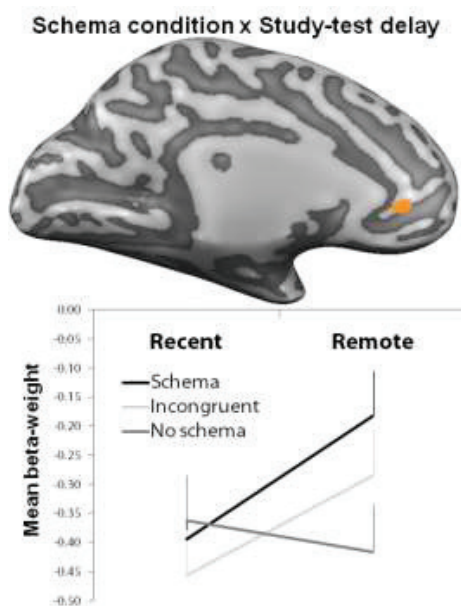
856 Figure 5



857

858 **Figure 5. Hippocampal deactivation during encoding of Schema quartets.** **a.** The blue overlay shows
 859 the posterior hippocampus area in which activity decreased parametrically for Schema quartets in
 860 the remote encoding session. Since the map shown is depicting a group-averaged, normalized,
 861 spatially smoothed overlay, voxels extend into the ventricle (6% overlap with the anatomical mask of
 862 the hippocampus). However, the peak voxel of the activation ($x = 23$, $y = -37$, $z = 13$, parametric
 863 decrease $t(23) = 4.398197$, $p < 0.001$) falls within the posterior hippocampus. In red (98% overlap
 864 with the anatomical mask of the hippocampus) the result from the PPI connectivity analysis with the
 865 AG as a seed region showing that the posterior hippocampus is modulated by the parametric
 866 increase of schema-related activity in the AG. Both maps are thresholded at a cluster-level corrected
 867 $p < 0.05$. **b.** The subject-averaged beta-weights from the hippocampal ROI showing the parametric
 868 decrease (represented by the blue blob in Fig. 5a) for each of the four objects in the quartet as a
 869 function of schema condition. In black Schema quartets, in light gray Incongruent quartets and in

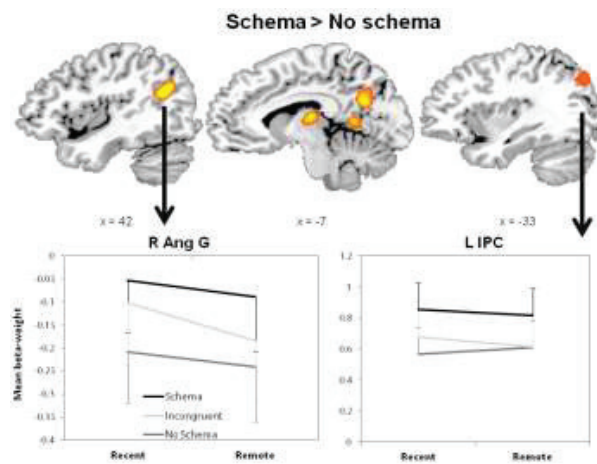
870 dark gray No schema quartets. **c.** Subject-averaged beta-values representing the parametric scores
871 of the hippocampal ROI that showed a parametric decrease in activity (represented by the red blob
872 in Fig. 5a) correlated with the amount of schema build-up in the AG. **d.** The PPI values from the
873 connectivity analysis from the AG to the hippocampus correlate with the amount of false alarms
874 participants made to the new Schema objects.

875 **Figure 6**

876

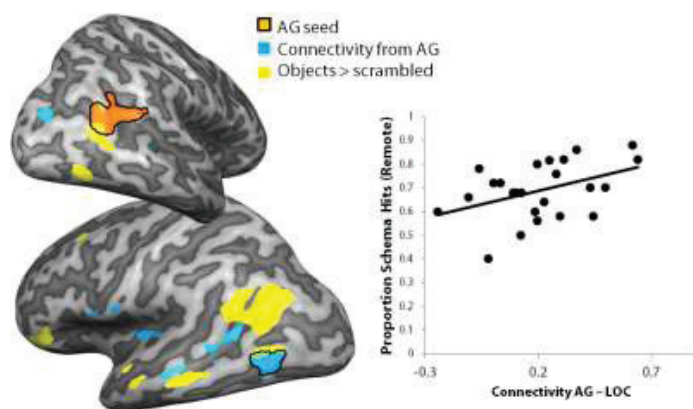
877 **Fig. 6. Study-test delay by schema condition interaction during retrieval.** We found a Study-test
 878 delay by Schema condition interaction in the right medial prefrontal cortex (mPFC, coordinates of
 879 the peak: $x = -6$, $y = 39$, $z = 2$, $F(1,23) = 26$, $p = 0.00004$, $SVC\ corr. < 0.05$) during retrieval. The mPFC
 880 result is presented on an inflated right hemisphere; dark gray colors represent the sulci. Plotted
 881 below are subject-averaged beta-weights extracted from all voxels within this mPFC region for
 882 Schema (black), No schema (dark gray), and Incongruent (light gray) remote and recent hits to
 883 provide information on the direction of the interaction and are shown here for this purpose (error
 884 bars reflect standard error of the mean).

885 **Figure 7**



887 **Fig. 7. Areas active during Schema retrieval.** The contrast between Schema and No schema objects
 888 (collapsed over time) was displayed as an overlay on three sagittal slices. The graphs below present
 889 the beta-weights from both ventral parietal areas (R Ang G, right angular gyrus and LIPC, left
 890 intraparietal cortex). Error bars represent the standard error of the mean.

891 **Figure 8**



892

893 **Fig 8. Angular gyrus connectivity during schema retrieval.** Connectivity from the angular gyrus (AG)
 894 seed region (in orange) was explored with a PPI analysis for remote Schema objects compared to
 895 remote No schema objects (overlay in blue). These results are overlaid on two inflated hemispheres
 896 and combined with the overlay (in yellow) from the functional localizer contrasting objects with
 897 scrambled objects. The right graph represents the correlations between memory performance
 898 (proportion of hits in the remote condition) and PPI connectivity scores for Schema objects as
 899 indicator of the strength of the psychophysiological interaction (PPI).

900

901 **Tables**

902

Area	x	y	z	t
<i>Parametric increase</i>				
R Middle Frontal G	30	17	31	5.40
Thalamus	12	-10	4	4.79
Parahippocampal G	-6	-61	4	5.47
L Inferior Frontal G	-30	32	19	5.56
L Angular G	-30	-67	37	5.91
L Superior Temporal G	-36	-25	10	4.72
<i>Parametric decrease</i>				
R posterior hippocampus	27	-40	10	-5.18

903

904 **Table 1. Schema build-up.** Areas modulated by the parametric regressor for schema build-up in the
 905 remote encoding session for quartets with a subsequently remembered final object. Coordinates are
 906 Talairach coordinates of the peak voxel. For all *t*-values (df = 23) *p* was < 0.0001.

907

Area	x	y	z	t
R Superior Temporal G	57	-1	4	4.51
Bilateral Parietal and Cuneus	9	-82	25	6.63
R Precentral G	33	-16	43	4.35
R Superior Frontal G	27	59	19	4.50
Precuneus	15	-46	40	5.46
L Inferior Occipital G	-6	-61	4	4.52
L Middle Frontal G	-30	53	10	5.98





















L Precentral G	-51	-22	40	5.03
L Postcentral G	-57	-22	22	5.07

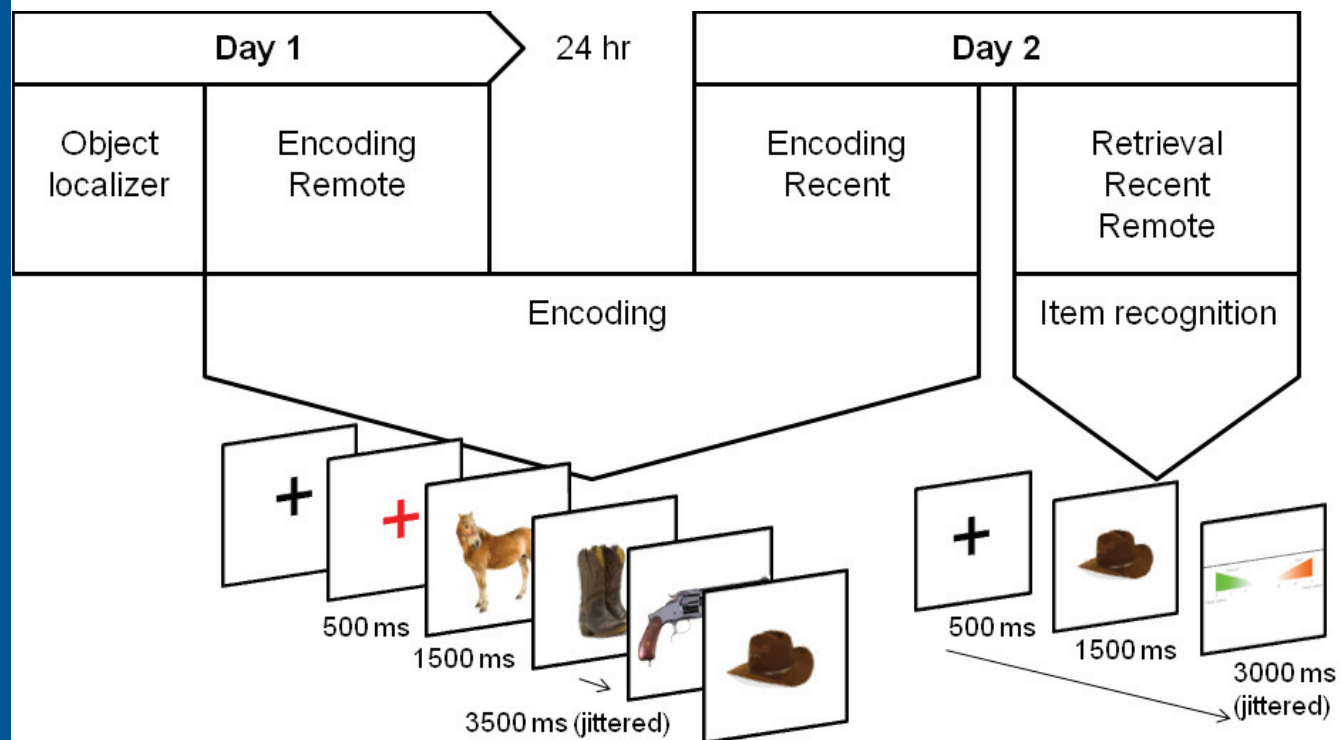
908

909 **Table 2. Parametric schema effect.** Areas that show a larger parametric build-up for Schema versus

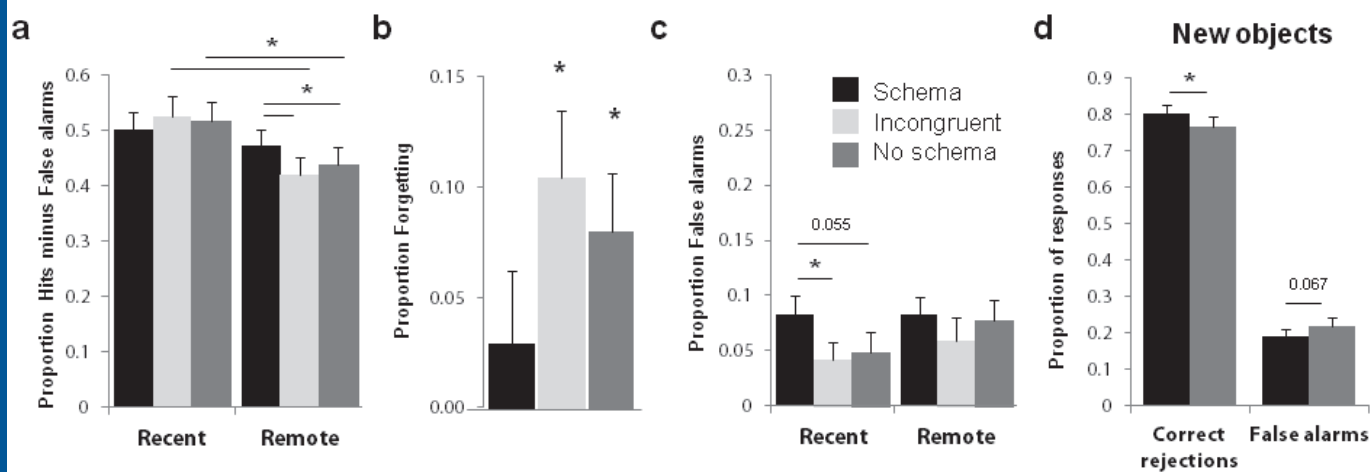
910 No schema quartets in the remote encoding session. Coordinates are Talairach coordinates of the

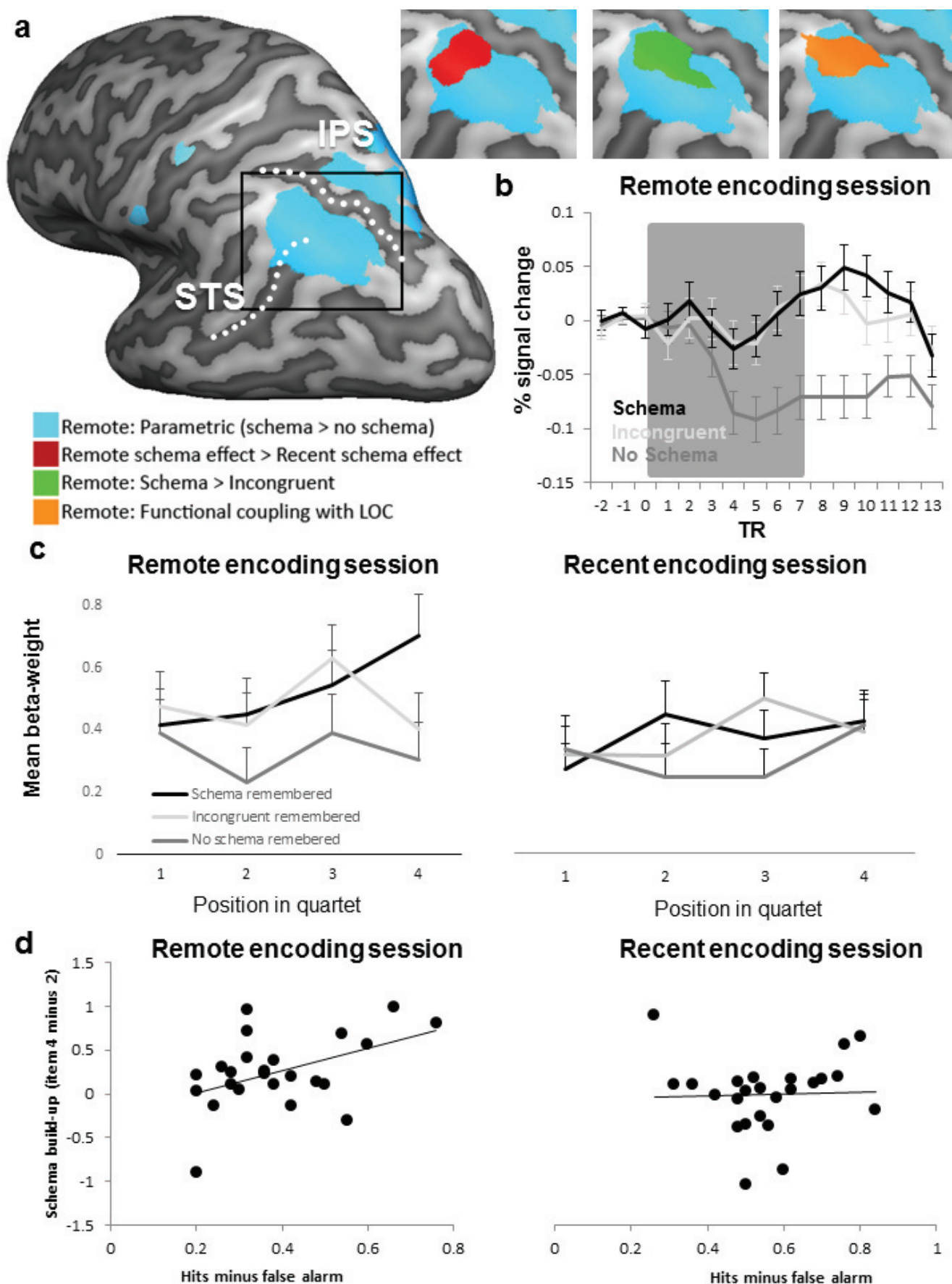
911 peak voxel. For all t -values ($df = 23$) p was < 0.001 .

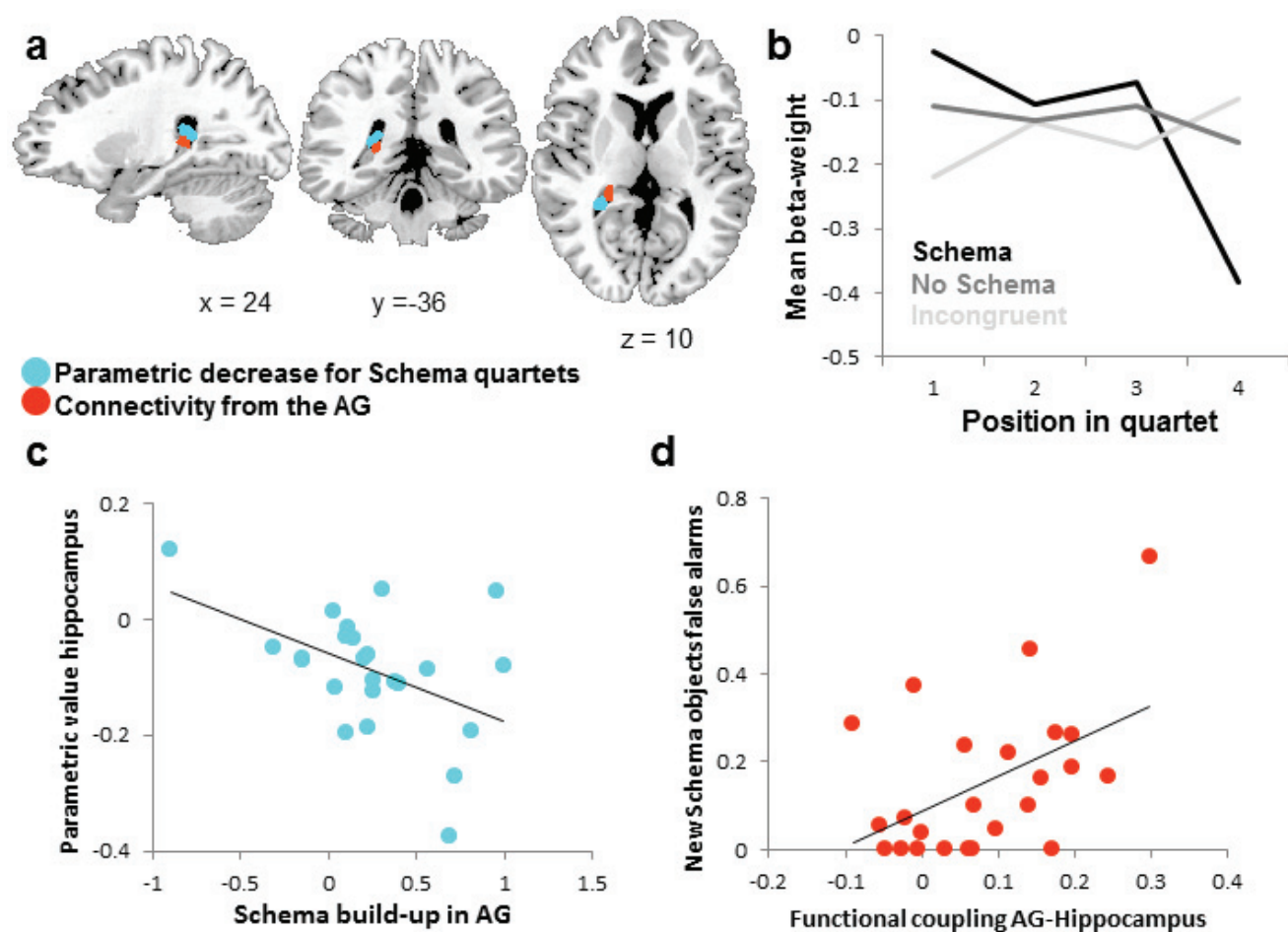
a.				b.		
Encoding				Item recognition		
1	2	3	4	Target	Lure	New
Schema						
						
No schema						
						
Incongruent						
						



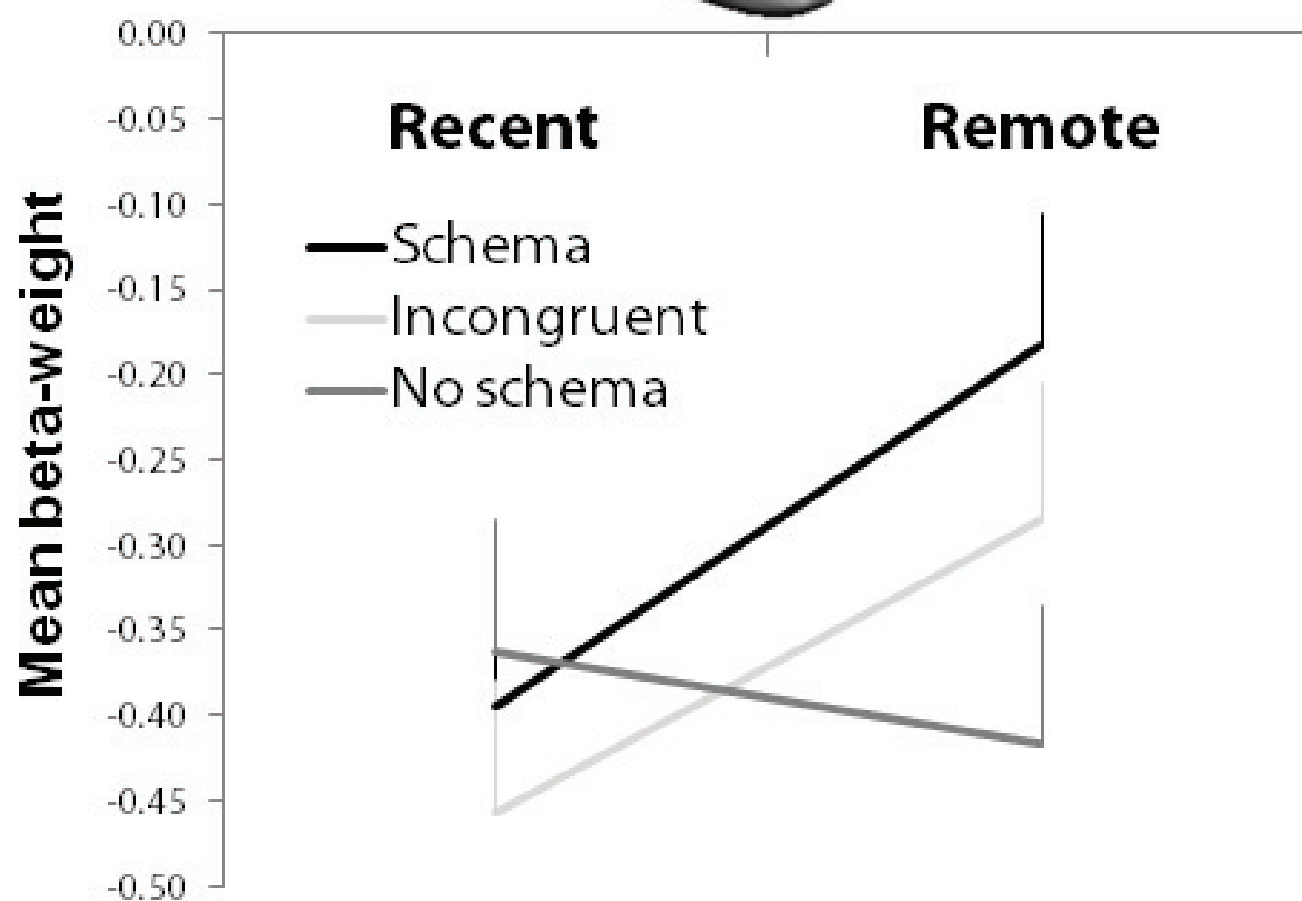
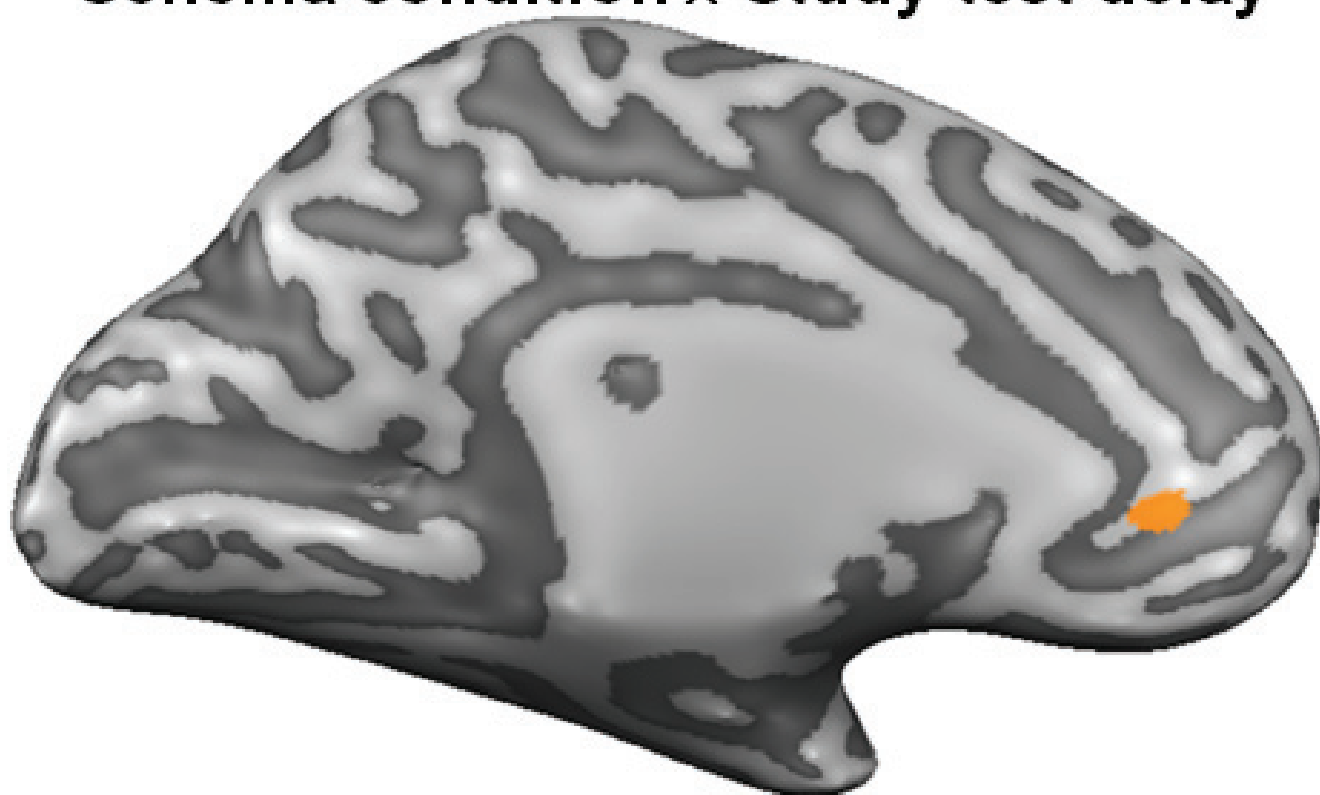
Item recognition conditions	New	Remote		Recent	
Schema	New	Target	Lure	Target	Lure
No schema	New	Target	Lure	Target	Lure
Incongruent		Target	Lure	Target	Lure



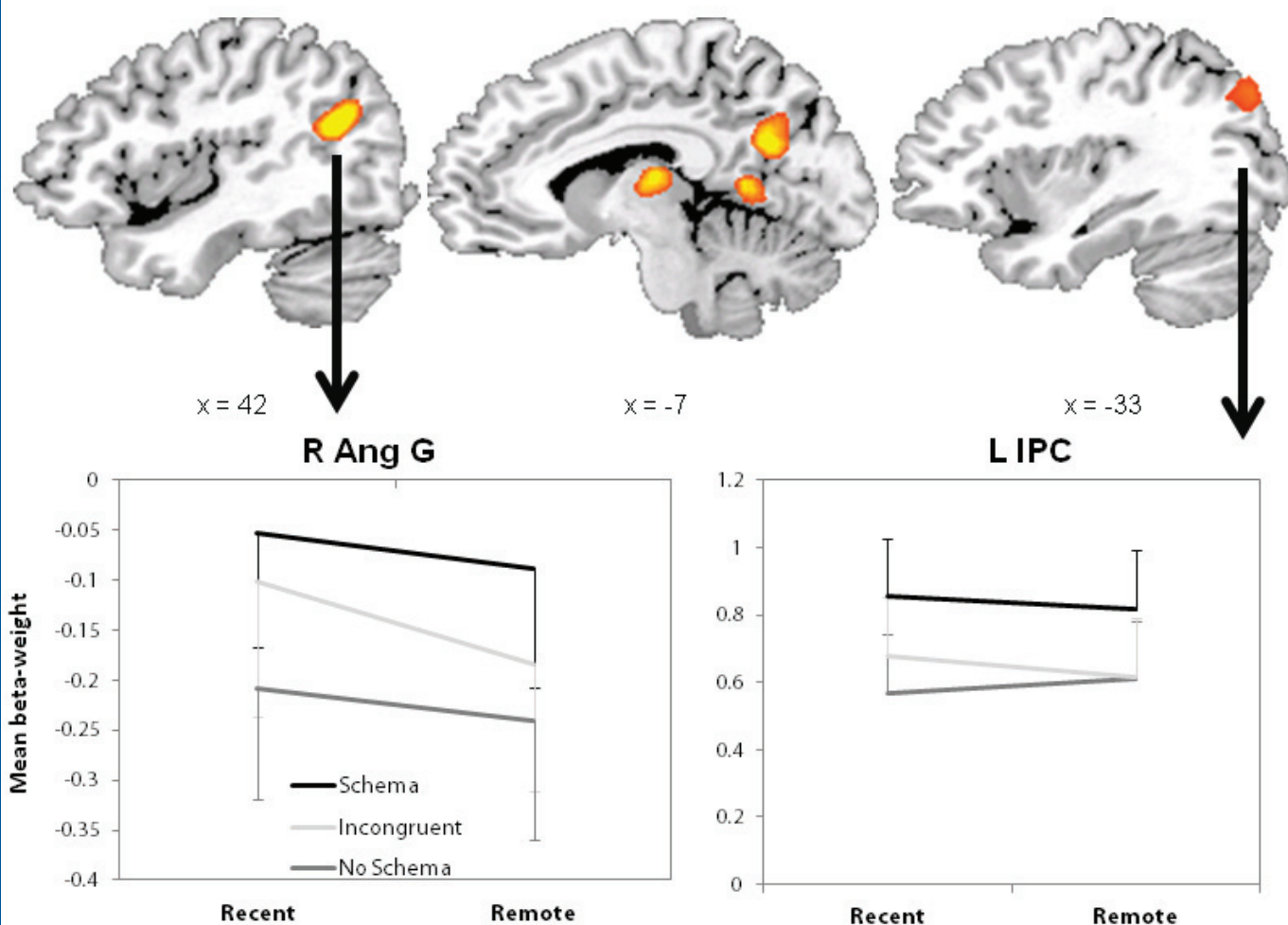


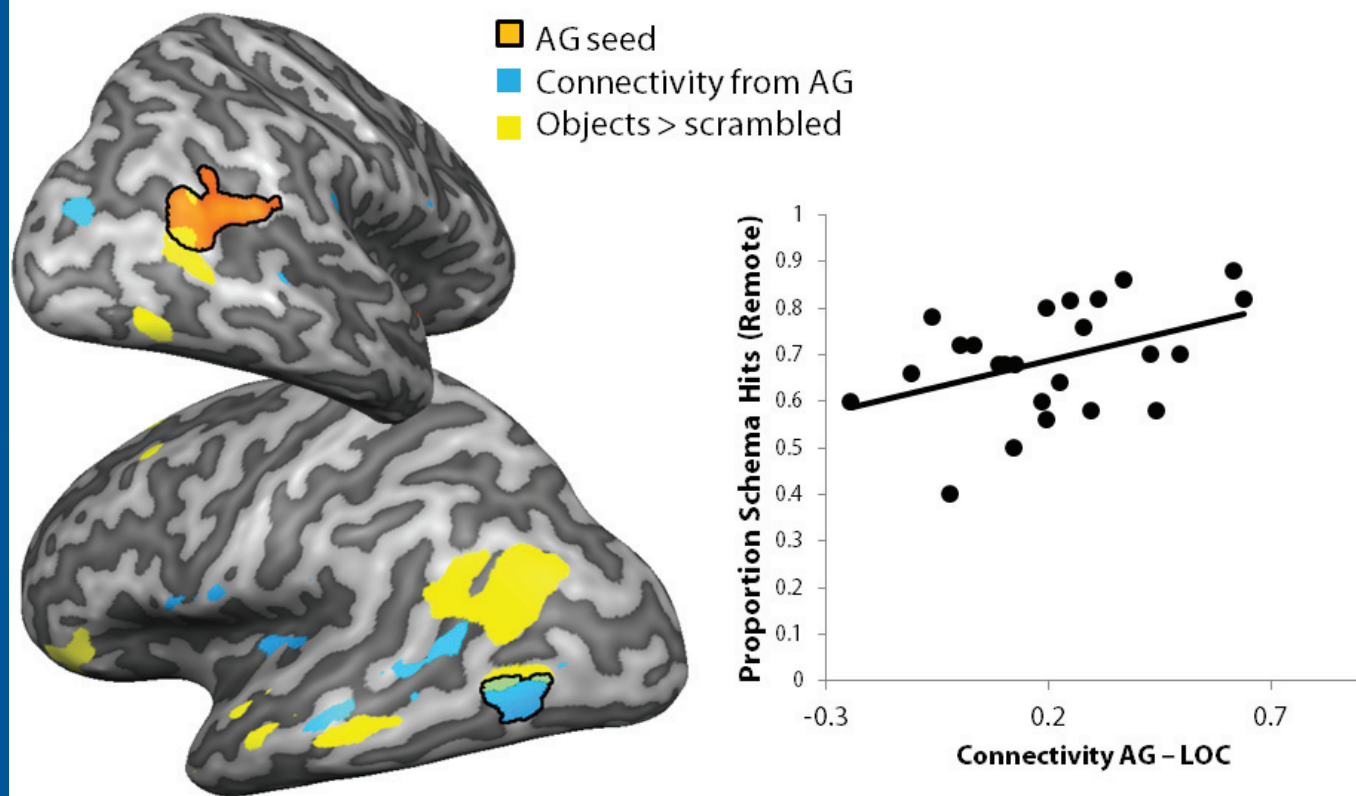


Schema condition x Study-test delay



Schema > No schema





Area	x	y	z	t
<i>Parametric increase</i>				
R Middle Frontal G	30	17	31	5.40
Thalamus	12	-10	4	4.79
Parahippocampal G	-6	-61	4	5.47
L Inferior Frontal G	-30	32	19	5.56
L Angular G	-30	-67	37	5.91
L Superior Temporal G	-36	-25	10	4.72
<i>Parametric decrease</i>				
R posterior hippocampus	27	-40	10	-5.18

Table 1. Schema build-up. Areas modulated by the parametric regressor for schema build-up in the remote encoding session for quartets with a subsequently remembered final object. Coordinates are Talairach coordinates of the peak voxel. For all *t*-values (*df* = 23) *p* was < 0.0001.

Area	x	y	z	t
R Superior Temporal G	57	-1	4	4.51
Bilateral Parietal and Cuneus	9	-82	25	6.63
R Precentral G	33	-16	43	4.35
R Superior Frontal G	27	59	19	4.50
Precuneus	15	-46	40	5.46
L Inferior Occipital G	-6	-61	4	4.52
L Middle Frontal G	-30	53	10	5.98
L Precentral G	-51	-22	40	5.03
L Postcentral G	-57	-22	22	5.07

Table 2. Parametric schema effect. Areas that show a larger parametric build-up for Schema versus

No schema quartets in the remote encoding session. Coordinates are Talairach coordinates of the peak voxel. For all t -values ($df = 23$) p was < 0.001 .